Computer Methods and Programs in Biomedicine 214 (2022) 106546

Contents lists available at ScienceDirect

Computer Methods and Programs in Biomedicine

journal homepage: www.elsevier.com/locate/cmpb

Computer modeling of radiofrequency cardiac ablation: 30 years of bioengineering research

Ana González-Suárez[a,b], Juan J. Pérez[c], Ramiro M. Irastorza[d,e], Andre D'Avila[f], Enrique Berjano[c,*]

[a] Electrical and Electronic Engineering, National University of Ireland Galway, Ireland
[b] Translational Medical Device Lab, National University of Ireland Galway, Ireland
[c] Department of Electronic Engineering, BioMIT, Universitat Politècnica de València, Valencia, Spain
[d] Instituto de Física de Líquidos y Sistemas Biológicos (CONICET), La Plata, Argentina
[e] Instituto de Ingeniería y Agronomía, Universidad Nacional Arturo Jauretche, Florencio Varela, Argentina
[f] Division of Cardiovascular Medicine, Beth Israel Deaconess Medical Center, Harvard Medical School, Boston, MA, United States

ARTICLE INFO

Article history:
Received 16 August 2021
Revised 8 November 2021
Accepted 15 November 2021

Keywords:
Bioengineering
Cardiac ablation
Computer modeling
In-silico model
Radiofrequency ablation

ABSTRACT

This review begins with a rationale of the importance of theoretical, mathematical and computational models for radiofrequency (RF) catheter ablation (RFCA). We then describe the historical context in which each model was developed, its contribution to the knowledge of the physics of RFCA and its implications for clinical practice. Next, we review the computer modeling studies intended to improve our knowledge of the biophysics of RFCA and those intended to explore new technologies. We describe the most important technical details of the implementation of mathematical models, including governing equations, tissue properties, boundary conditions, etc. We discuss the utility of lumped element models, which despite their simplicity are widely used by clinical researchers to provide a physical explanation of how RF power is absorbed in different tissues. Computer model verification and validation are also discussed in the context of RFCA. The article ends with a section on the current limitations, i.e. aspects not yet included in state-of-the-art RFCA computer modeling and on future work aimed at covering the current gaps.

1. Introduction

Radiofrequency (RF) catheter ablation (RFCA), also known as RF cardiac ablation, is a minimally invasive procedure that can cure cardiac arrhythmias by using RF electrical energy to cause irreversible thermal destruction of the arrhythmia focus or create linear lesions to block the conduction of action potentials associated with arrhythmia. Fig. 1 shows the overall scenario during RFCA, when an intravascular catheter is introduced until it reaches the target site in the heart. Once there, RF power is applied through a metal electrode at the catheter tip (active electrode). RF current circulates between the active electrode and a large dispersive electrode on the patient's skin (usually back or thigh). Although RFCA can be considered a standard procedure in the context of minimally invasive cardiology, it uses highly complex medical technology, since ablation catheters, apart from mapping, stimulating and delivering RF energy, have been increasingly equipped in recent years with technical improvements, such as sensors for temperature and contact force, external/internal saline irrigation, and elements to assist in navigation and guidance. In fact, the ever-increasing demand to achieve thermal lesions closely circumscribed to the target and avoiding damage to nearby tissues (e.g. the esophagus), and simultaneously avoiding overheating in the tissue (steam pops) and blood (thrombi) forces us to rethink the complexity of the physics involved around the RF electrode in a real clinical scenario, which could be described in the following terms of uncertainty: a small metal electrode (3.5 – 4 mm long, 7 – 8Fr in diameter) at the tip of a vascular catheter contacts the endocardium surface at a not fully controllable angle (ranging from vertical to horizontal), with an insertion depth not totally controllable (which is related to the contact force and irregularity of the endocardial surface, e.g. trabeculae), on an area of tissue that can present a variety of different electrical and thermal characteristics (changing drastically during heating and depending on the individual patient, the intramyocardial capillary blood flow, pathological state of the substrate, proximity to previously

* Corresponding author: Department of Electronic Engineering, BioMIT, Universitat Politècnica de València, Building 7F, Camino de Vera, Valencia 46022, Spain.
E-mail address: eberjano@eln.upv.es (E. Berjano).

https://doi.org/10.1016/j.cmpb.2021.106546

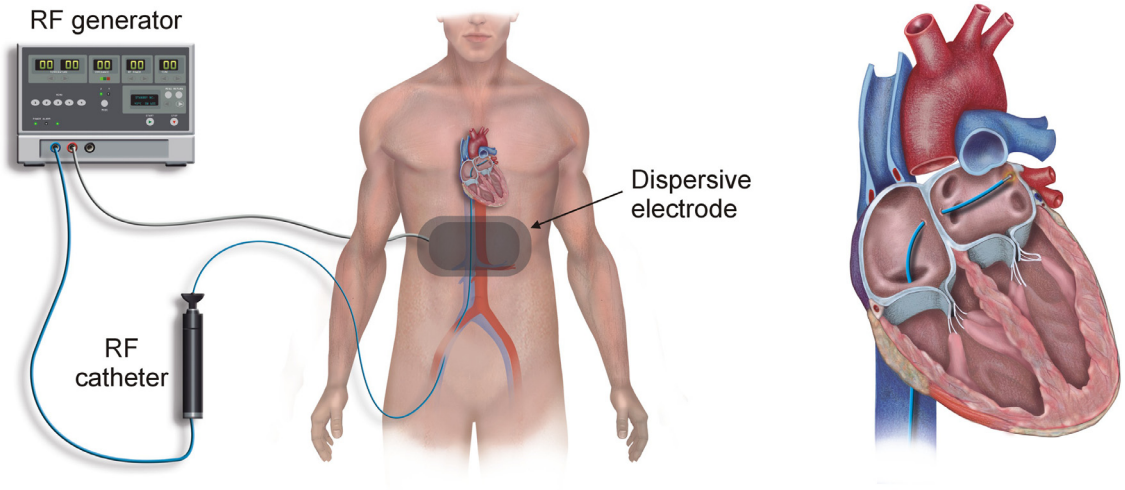

Fig. 1. Radiofrequency cardiac ablation (RFCA) consists of introducing an intravascular catheter until it reaches the target site. RF power is then applied through a metal electrode at the catheter tip (active electrode). RF current circulates between the active electrode and a large dispersive electrode on the patient's skin, causing the irreversible thermal destruction of the cells causing the arrhythmia or blocking the conduction of action potentials associated with arrhythmia (in case of linear lesions in the atrial fibrillation ablation).

ablated areas or medium/large vessels, etc.), surrounded by a circulating blood flow that can vary widely depending on the location within the chamber (and hence altering the heat evacuation conditions from the tissue surface and the electrode itself), and with the aim of delivering RF current that travels through very different tissues in the torso (with very different electrical properties, such as blood vessels, bones, lung, etc.) until completing the electrical circuit through a dispersive electrode on the patient's skin (in the monopolar mode). To sum up, a scenario characterized by many uncontrolled variables which surely have an important effect on the lesion characteristics and geometry. And despite the extremely high complexity of the physical scenario, mathematical and computational modeling (also known as *in-silico* trial) is still valuable, possibly due to having the potential to simulate the behavior of some aspects of RFCA while keeping most of the variables under control. In other words, while theoretical modeling may lack the realism of a clinical setting, it can suggest answers to the complex questions to be solved by experimental or clinical studies. It should thus be considered as a complementary tool to experimental studies.

This article reviews the theoretical, mathematical and computational RFCA models developed to date, emphasizing their historical context, contribution to the RFCA physics and their possible implications for clinical practice. We point out some aspects not yet included in the state of the art of RFCA modeling, which will surely require further studies to cover the existing gaps in our knowledge. As far as we are aware, this is the first review exclusively focused on RFCA computer modeling, even though previous reviews have dealt with RF ablation computer modeling for different medical purposes, especially for RF tumor ablation [1,2]. Some excellent articles have been published to date describing the physics involved in RFCA [3–5]. Fig. 2 graphically summarizes the main physical phenomena involved in this process and hence the problems to be solved by computer modeling.

Recently, attention has been paid in two additional physical problems; one is the fluid dynamics problem associated with the movement of blood within the cardiac chamber and its possible interaction with saline through the holes in tip-irrigated catheters. In this case, computer modeling has focused on predicting the temperature in the blood around the RF electrode, which is known to be related to the appearance of thrombi. The other is the mechanical problem underlying the deformation of the myocardium surface by the force applied by the electrode, especially the contact force (CF), as a determining factor in lesion size.

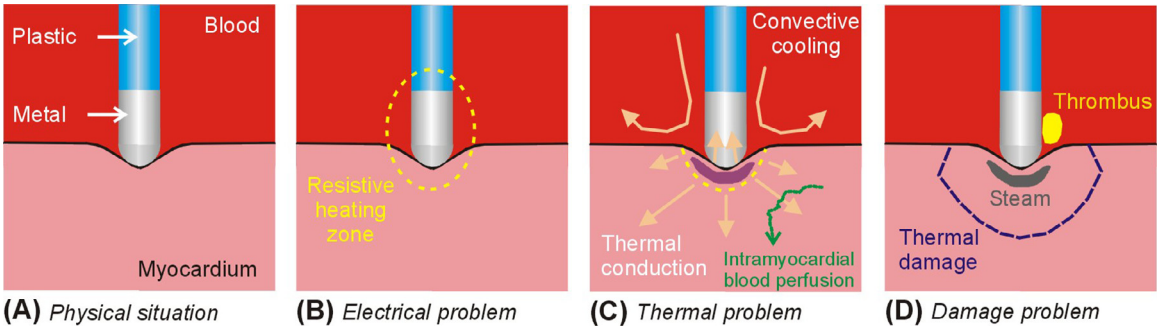

Fig. 2. A: The physical situation is simplified by assuming that the catheter is vertical and induces an indentation on the myocardium surface. **B:** Solving the electrical problem involves calculating the electrical power absorbed around the electrode (this power is converted to heat by the 'Joule effect'). **C:** The thermal problem takes into account all the mechanisms associated with heat flow, such as thermal conduction through tissue and electrode, heat losses by intramyocardial perfusion and convective cooling caused by circulating blood, as well as thermal energy storage in the form of a temperature change. **D:** The thermal lesion contour can be estimated from the computed temperature and exposure time using different injury models, such as the Arrhenius' damage model. The maximum temperature reached in tissue and blood can also suggest the possible occurrence of steam pops or thrombi.

2. Review of previous studies

2.1. Historical perspective

Fig. 3 shows a timeline with some of the most representative theoretical (analytical/computational) models from 1989 to the present.

The first theoretical model was proposed by Haines and Watson [6], when RFCA was a relatively new procedure and little was known about how lesion size and geometry were determined. This study used a simplified three-dimensional model to analyze the energy equilibrium at each volume differential to balance the 'Joule effect' and thermal conduction as a function of the distance r to the electrode. Since it presented radial symmetry it was analytically resolved in a single dimension. The goal was to predict the temperature profile around a spherical RF electrode completely immersed in a homogeneous and infinite medium that mimicked the cardiac tissue. The electrical problem was analytically solved resulting in a spatial distribution of power with the maximum on the electrode surface and a steep drop (proportional to $1/r^4$) away from the electrode. This suggested that the conversion of electrical power to heat by the 'Joule effect' was limited to a narrow rim around the electrode, so that this zone could thus be acting as a heat source creating the lesion mainly by thermal conduction. From then on they assumed a steady state, which made sense if the electrode temperature remained constant (note that at that time electrical power was usually modulated to keep the electrode temperature constant). Using the law of Fourier's heat conduction, they then obtained a mathematical expression to predict the temperature profile around the RF electrode from its radius and the temperature on its surface (which remained constant during the ablation, ~120 s, long enough to reach a steady state). The model was later validated by *ex vivo* experiments [7] and showed a strong linear correlation between electrode radius and lesion radius when RFCA was conducted with a temperature-control mode (60 °C) for a relatively long time (90 s).

A few years later, in 1994, Labonté proposed the first computational model that included a more or less realistic scenario consisting of an ablation electrode on a fragment of tissue [8]. Its most innovative feature with respect to the Haines and Watson model was the inclusion of blood around the electrode. This significantly affected both the electrical problem (since most of the RF current flowed through the blood and not through the tissue) and the thermal problem (since the moving blood cooled the tissue and electrode surface, which was modeled assuming convection coefficients at the blood-tissue and blood-electrode interfaces). The electrode was assumed to be perpendicular to the tissue, which meant a two-dimensional model could be solved (thanks to the rotational symmetry with respect to the catheter axis). Due to the complex geometry used, an analytical solution was not feasible and a numerical method, such as the Finite Element Method (FEM), was used to solve the coupled electrical-thermal problem. Labonté's model was the first to use the Bioheat Equation as the governing equation for the thermal problem, thus solving a transitory problem, as opposed to the Haines and Watson model which solved the steady state, as well as the Arrhenius damage function to quantify the lesion size in the cardiac tissue. The model was experimentally validated on an agar phantom and thermographic imaging, showing the predicted ellipsoidal lesions similar to those previously found in experimental studies. In terms of biophysics, Labonté's model clearly illustrated the phenomenon by which RF exclusively heats the tissue while the electrode remains cooler and really acts as a heat sink, keeping the temperature distribution inside the tissue and thus provided larger lesions than those obtained by a hot-tip catheter of the same size [9]. Precisely thanks to this factor, the model predicted that lesion size increased not only with the electrode radius (as predicted by Haines and Watson's model), but also with its length because of the larger convective losses of the blood flow. It also pointed out that these convective losses could cause a large temperature difference between electrode and tissue, which could be a problem in temperature-controlled ablations in which power is modulated to keep the temperature approximately constant in the electrode. In fact, the position of the temperature sensor in the catheter is known to be critical in these cases [10].

Also in 1994, Sahidi and Savard proposed a concentric sphere model that included not only cardiac tissue and blood, but also a simplified torso and a dispersive electrode on its outer surface [11]. This model was used to suggest that lesion size was not sensitive to the dispersive electrode's position. This same model was later used to study the effect of different factors on lesion size, such as blood flow, the electrode length and its thermal conductivity [12].

In 1995, Prof. Webster's group at the University of Wisconsin in Madison proposed the first three-dimensional model, which considered two realistic electrode geometries [13] (note that the pre-

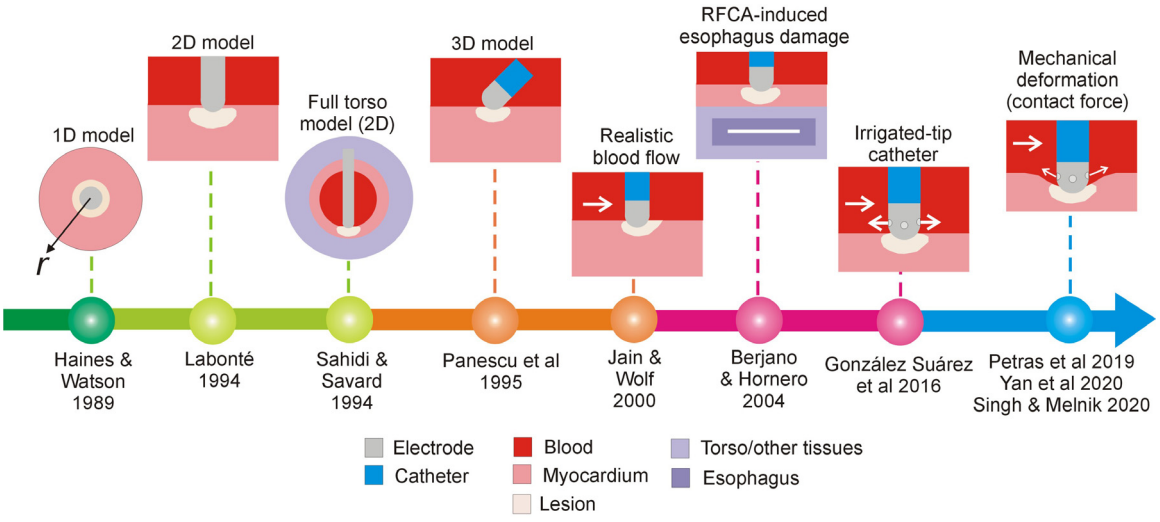

Fig. 3. Timeline with some of the most representative theoretical (analytical / computational) models from 1989 to the present. The models progressively incorporated the contiguous tissues (e.g. torso, esophagus) as well as a greater degree of detail (e.g. blood movement and external irrigation of the electrode –white arrows–, mechanical deformation of the endocardium, etc.).

vious model by Sahidi and Savard assumed axial symmetry, considering only a 10° slice and hence solving a 2D problem). This first 3D model could study the effect of the catheter/tissue angle (perpendicular, 45° and horizontal) on lesion size. In the following years, this group conducted several interesting studies with 2D and 3D models to analyze the electrical and thermal performance of different electrode geometries [14,15] and the effect of changes in tissue properties [16]. These models were also used to predict lesion size according to the target location inside the cardiac chamber [17,18] and to assess technical improvements to achieve long, continuous transmural lesions in the context of atrial fibrillation (AF) ablation [19].

Also around the same time (1998−2000), Jain and Wolf of the Duke University conducted meticulous computer modeling studies combined with *in vivo* and *ex vivo* models [20–22] particularly focused on the effect of the dispersive electrode on lesion size. Their 3D model published in 2000 was really the first to solve the fluid dynamics associated with the blood flow and hence obtained a realistic temperature distribution in the blood around the electrode [22]. Note that up to that time, the thermal convection effect of circulating blood had been modeled using the heat transfer coefficients set at the electrode-blood and tissue-blood interfaces. The computational results for the first time offered an asymmetric lesion due to the directional blood flow.

In 2001 Demazumder et al. [23] published the first RFCA computer model using an irrigated electrode. Although they did not solve the fluid dynamics associated with the saline infusion, they did propose a simplified method based on keeping the electrode temperature constant to a value similar to that measured on the same electrode in experimental studies. This simplification was also used in later modeling studies of irrigated-tip catheters by setting a value of 45 °C in the cylindrical zone of the electrode tip and leaving the semispherical tip free [24–26] (this value was suggested from the mean value measured at the electrode tip during *ex vivo* ablations [27]). Later, in 2005, Berjano and Hornero used 3D computer models to assess different issues related to the esophageal injury associated with RFCA on the posterior atrial wall [28–30].

In the last 15 years several groups have carried out RFCA studies based on computer modeling which gradually incorporated new realistic details, such as the interaction between the blood flow and the saline injected by irrigated-tip catheters [31,32] and the mechanical deformation of the tissue surface due to the contact force [33–35] (note that although the model by Cao et al. [36] in 2002 considered a realistic deformation of the tissue surface, it did not consider its relationship to the contact force or its effect on lesion size).

2.2. Computer modeling to obtain further information on the biophysics involved

As Wittkampf and Nakagawa pointed out, although the results of computer modeling must not change the daily practice of RFCA they can provide an understanding of what happens during ablation [37]. Computer modeling should therefore be considered as a complementary tool to experimental studies, which are really an irreplaceable means of validating computational results. Computer modeling has clear advantages: 1) the variables can be kept under control and assigned ranges of individual or multiple variations: and 2) it can analyze thermal and electrical variables in areas very close to the electrode, where in fact they change so drastically with distance (i.e. huge gradients) that they are impossible to map experimentally.

The Labonté study conducted in 1994 is one of the best examples of computer modeling that facilitated an understanding of RFCA biophysics [9], since it clearly illustrated the differences between the spatial distribution of electrical power (also known as Specific Absorption Rate, SAR) absorbed around the electrode in both blood and tissue, and the thermal lesion created exclusively in the tissue. The lesion shape is typically ellipsoidal with the hottest point slightly displaced from the electrode surface, which acts as a heat sink. Fig. 4 shows the typical electric field distribution around the electrode for two catheter angles (perpendicular and parallel) and the resulting temperature distribution in blood and tissue. The value of the electric field is directly related to the electrical power deposited, and as can be seen, it is limited to a narrow area around the electrode, most markedly at the edge where the metal meets the plastic. Interestingly, it is greater around the spherical tip than around the cylindrical surface. The physical explanation for this is that the electric field decays approximately at a rate of $1/r$ around the cylindrical zone of the electrode and $1/r^2$ around the spherical zone, i.e. the tip (see axis r in Fig. 4A,B). Note that these ratios are mathematically true only when a cylinder of infinite length and a complete sphere are considered, respectively. This means that more electrical power is deposited around the spherical zone (since it decays at a rate of approximately $1/r^4$ [6]) than in the cylindrical zone (where it decays at $1/r^2$). This different power deposition profile around the electrode depends on the area (spherical vs. cylindrical) that could favor the creation of deeper lesions by horizontal electrodes.

Fig. 4C,D shows the temperature distributions in myocardium and blood. Although the electrical power is deposited both in blood and myocardium (see Fig. 4A,B) the temperature rise and thus the lesion is only in the myocardium since the blood flow evacuates the heat and cools the myocardium surface making an ellipsoidal lesion, as was found in experiments [27]. In addition, the hottest point in the myocardium is not far from the electrode tip since the electrode body acts as a powerful heat sink thanks to a thermal conductivity around 100 times greater than that of the myocardium. The computer results thus show that RF current does not directly heat the electrode, but only a very thin rim of contiguous tissue, and then the electrode is heated in turn by thermal conduction from the tissue, evacuating heat towards the circulating blood. In fact, the thermal effect of blood flow drastically affects lesion size by evacuating power from the area of tissue heated by RF [17]. As a general rule, the thermal lesion is expected to be created at the points with high values of electrical power and where there is little heat evacuation. While the computer results confirm that the SAR is maximum at sharp geometric gradients (e.g. at the point where the electrode and the plastic part of the catheter meet, or at the tip of needle-like electrodes [15]), thermal damage will only occur if there is no heat evacuation. So, circulating blood avoids heating at the electrode-catheter junction in the case of a vertical catheter angle (see Fig. 4C), however there are hot points at these junctions (due to the edge effect) when the catheter is horizontal (see Fig. 4D) [31] or with long electrodes resting completely on the tissue [38]. The position of these hot spots on the temperature maps obtained from computer simulations can suggest where the temperature sensors should be optimally placed on the catheter.

Berjano and Hornero conducted another computer modeling study to assess the impact of anatomical and procedural factors on the thermal damage in the esophagus [28]. They proposed a three-dimensional model including the tissues around the atrial wall (epicardial fat layer, esophagus, aorta, lungs, etc.). Their computer results suggested that the electrical power directly applied to the esophagus was insignificant and hence the esophageal injury was exclusively due to thermal conduction from the atrial wall. It was also found that the most important factor was the esophagus-electrode distance, which prompted clinical groups to mechanically separate the esophagus from the atrium during ablation [39]. A similar study was recently conducted with irrigated-tip catheters [32]. These studies are good examples of how computer models

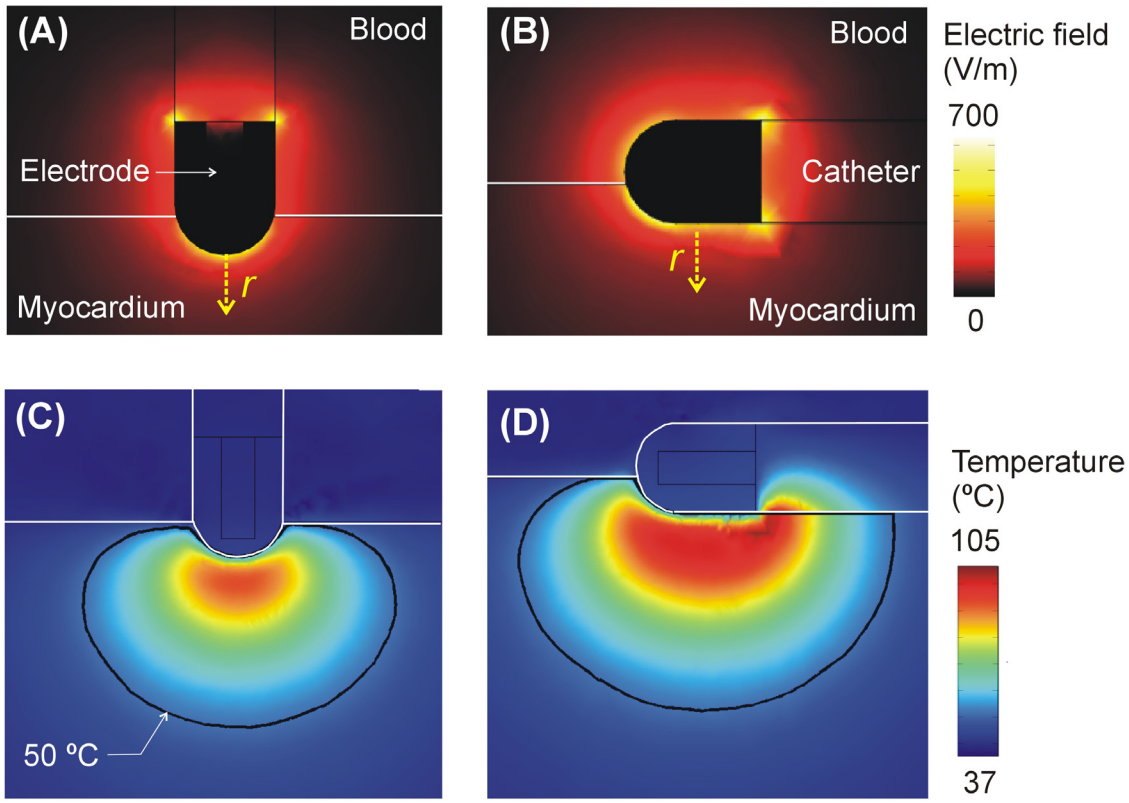

Fig. 4. Electric field (in V/cm) and temperature distributions (in °C) computed around the electrode during RFCA for perpendicular (**A,C**) and parallel (**B,D**) catheter. [*Results obtained on COMSOL Multiphysics (Burlington, MA, USA) a model of irrigated-tip catheter as described in [31]*].

can be used to analyze the factors causing the collateral damage and accidents associated with electrical and thermal phenomena, since they can compute the total volume of thermally damaged esophagus (see Fig. 5).

Perez et al. [25] is another example of a study aimed at understanding the biophysics of RFCA, particularly focused on scar-related ventricular tachycardia. They assessed the differences in lesion size created on normal myocardium and scar. Both tissue types were modeled from the electrical characteristics measured in previous experimental studies. The study concluded that although differences in tissue type may affect the density of electrical current on a small-scale, overall this does not appear to significantly impact lesion size. The computer results from this study showed the current density distribution across a heterogeneous tissue composed of ventricular myocardial, fat and fibrotic tissue, which is impossible to map in experimental studies. It was clearly seen that electrical current flows preferentially through tissues with higher electrical conductivity, i.e. through fibrotic tissue instead of fat, and viable myocardium instead of fibrous tissue. The Appendix provides a physical explanation of this phenomenon in terms of the electrical boundary conditions of an electric field [40].

Even though the first theoretical model proposed by Haines and Watson [6] suggested that lesion size is unaffected by the intramyocardial blood flow (and in fact most later computer models ignored the term of the Bioheat Equation representing blood perfusion), Perez et al. [26] revisited this issue in 2018 by using perfusion values reported in a data base, in particular an average value of 1026 ml/min/kg (obtained from the ITIS tissue properties database [41]) instead of 200 ml/min/kg (used in some previous computer modeling studies [11,42]). The results showed that intramyocardial blood flow can in fact affect lesion depth (a ~1 mm reduction) in long ablations (>1 min) such as those conducted on the ventricular wall. This is another example of how theoretical modeling can strictly control the value of some parameters and analyze their impact independently.

Thermal latency, which makes the lesion continue to grow deeper even after RF ablation, is another phenomenon involved in the physics of RFCA that has become more relevant in recent times (especially due to the use of RF power short pulses). This phenomenon was first studied by Wittkampf et al. in an *in vivo* model [43]. In 2018, Irastorza et al. [44] studied this phenomenon by computer modeling and quantified the increase in lesion size for different RF pulse durations: the shorter the pulse duration (keeping energy constant) the greater the lesion depth during the post-RF period. For instance, they reported that lesion depth can increase by 17% after a 10-s pulse and by up to 37% after an ultra-short RF pulse of only 1 s.

Most RFCA procedures use the monopolar mode, which means that RF current flows between the active electrode on the catheter tip and a large dispersive electrode on the patient's skin. Although this current flows through different types of tissue, from endocardium to skin, the current density is only high in the vicinity of the active electrode, so that only there can it potentially cause a rise in temperature (see Fig. 4). Although the temperature does not increase in the other types of tissue, dissipated RF power is in fact present in them. Fig. 6 shows the spatial distribution of the electrical variables involved in RFCA across the torso: electric field, voltage and SAR. Note that the SAR is especially high around the ablation electrode and the edges of the dispersive electrode, while it is very low in bony tissues. A recent computer modeling study included the full torso to estimate the percentage of RF power that is dissipated in tissues far away from the electrode and found a value of around 20% [45]. This estimation can be useful in adjusting the applied power in any limited domain model, such as computer models and *ex vivo* setups which do not include the full torso but only a fragment of tissue and blood around the electrode.

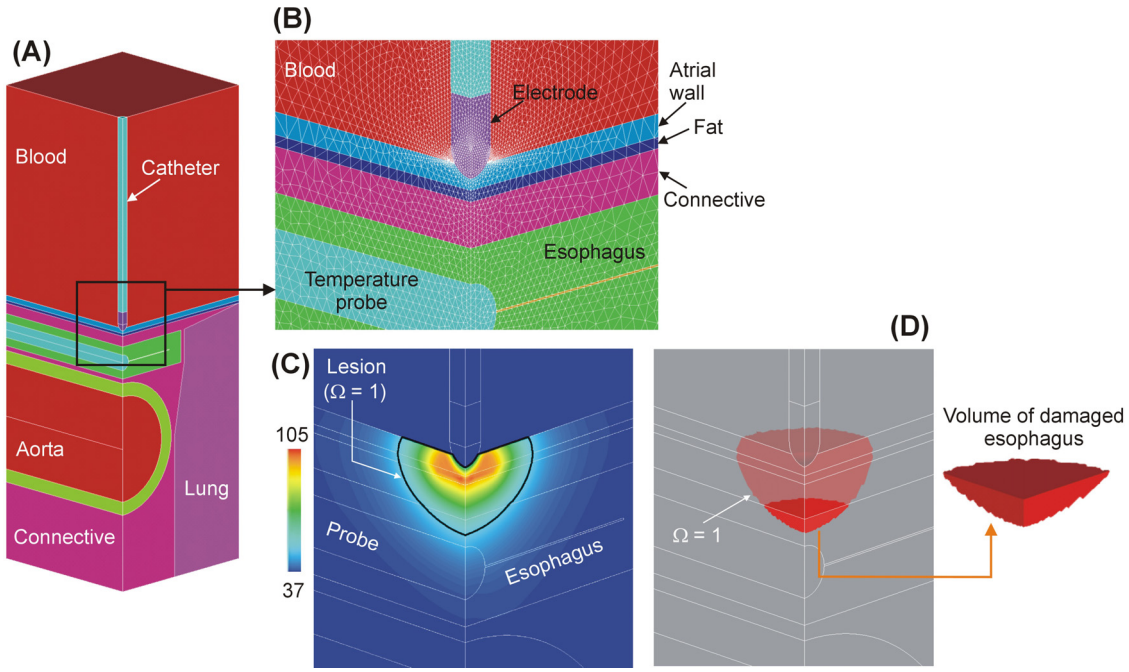

Fig. 5. A: 3D computer model including the tissues around the atrial wall (epicardial fat layer, esophagus, aorta, lungs, esophageal temperature probe, etc.) to analyze the factors causing thermal damage in the esophagus, **B:** Detail of the meshing, which is extremely fine at the electrode-tissue interface since this is where the greatest gradient in electrical and thermal terms is expected here. **C:** Temperature distributions in the tissues ($\Omega = 1$ is computed from the Arrhenius damage model and represents the lesion boundary). **D:** By selecting the 'esophagus subdomain', the total volume of thermally damaged esophagus can be estimated. [*Results obtained from ANSYS (Canonsburg, PA, USA)*].

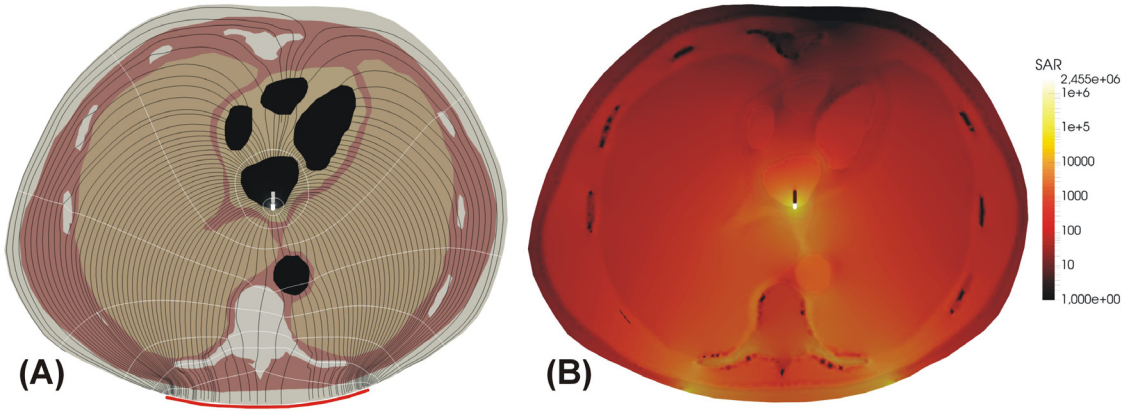

Fig. 6. A: Electrical field lines (black) and equipotential lines (white) computed across the tissues comprised in the torso. Red line represents the dispersive electrode. **B**: Electrical power dissipated in the tissues (also known as Specific Absorption Rate, SAR) (logarithmic scale). [*Results obtained from FEniCS* (https://fenicsproject.org)].

2.3. Computer modeling to explore new RFCA systems

Computer modeling is now an important aid in the research and development of RFCA technology. As Panescu et al. [13] pointed out, since it is difficult to obtain good spatial resolution when measuring the actual current densities and temperatures within the tissue near the electrode experimentally, it seems preferable to model significant cases initially and then confirm the computer results with experimental data. In fact, the preliminary computational results could suggest improvements in the design of preliminary experiments. Thanks to this advantage, as well as its speed and low costs, computer modeling has been used as a proof of concept for the development of technical improvements related with electrode design. For example, needle-like electrodes have been developed to achieve deep lesions in the ventricular wall [15], as well as new shapes and materials to join electrodes and catheters to reduce the hot points in this zone [14] and different metal materials to achieve better heat evacuation through the electrode body and increase lesion size [46]. Computer modeling has also been used to explore the performance of different modes of applying RF energy, such as constant temperature [9,21,47], constant power [21], and high power in short durations [48–50].

In the context of atrial fibrillation ablation, in which continuous (without gaps) long transmural (sufficiently deep) lesions are sought, computer modeling has been used to compare different ways of applying RF energy (monopolar or bipolar) using several electrodes on the same catheter [51,52], in particular by using suitably phase-shifted voltages [19,53] or changing the duty cycle (duration in which each electrode is active in relation to the total application time) [54]. It was also used to assess the impact of an occlusion balloon in an epicardial vessel to temporarily stop the

blood flow and facilitate the creation of transmural lesions across the atrial wall during mitral isthmus RFCA [55]. The performance of irrigated-tip catheters has been studied by including fluid dynamics in the computer modeling, obtaining realistic temperature distributions in the electrode-blood interface [31], which is related to the risk of the formation of thrombi.

In the context of ventricular tachycardia ablation, where the target is often in deep positions, computer modeling has explored alternative techniques to create deeper lesions. For instance, a computer model was proposed to compare the effectiveness of bipolar and unipolar modes in terms of creating transmural lesions across the interventricular septum and ventricular free wall using two catheters on opposing sides of the ventricular wall [56]. Note that in the case of a free wall, the catheter on the epicardial side is not in contact with circulating blood, so that the electrical and thermal conditions are therefore very different from endocardial ablations. In fact, several computer models have also been proposed to study temperature distributions during epicardial RF ablation [57–59]. They have also studied the geometry of lesions inside the ventricular wall using specific electrode designs such as needle-type electrodes [15] and an RF-energized guidewire inserted into the ventricular wall [60].

Other studies have evaluated novel techniques for thermal protection of the esophagus during AF ablation, such as probes that actively cool the esophagus [29,61,62]. Some studies analyzed the procedural problems associated with the position of the probe with respect to the ablation point when using esophageal temperature probes [30], and assessed the electrical and thermal interference induced by different types of commercially available temperature probes, especially those whose temperature sensors have a metal surface [24].

Gonzalez-Suarez et al. [63] used computer modeling to analyze the relationship between the 50 °C and 70 °C isotherms, which are related to irreversible thermal lesions and the loss of birefringence due to fiber denaturation, respectively. The aim was to explore the feasibility of a new catheter able to conduct measurements by polarization-sensitive optical coherence reflectometry (since changes in accumulated phase retardation occur around 70 °C) to estimate lesion size (which occurs around 50−55 °C) in real-time.

Computer modeling has also been used recently by Verma et al. [64] to study the temperature distributions created by a diamond-tipped catheter and explore its enhanced heat removal potential over platinum-iridium electrodes. To sum up, computer simulation allows you to quickly and reliably explore any hypothesis on technical improvements and innovations in RFCA and the results can be used to reject those that do not provide advantages while those that do can be verified experimentally.

2.4. Computer modeling for cardiac ablation based on other energies

Although RF is energy normally in RFCA, other energies have been studied as possible alternatives, such as microwave [65,66] and High-Intensity Focused Ultrasound (HIFU) [67,68]. Cryoablation and laser applied by means of a balloon are currently an alternative to RF in pulmonary vein isolation to treat atrial fibrillation [69]. Hot balloons have also been used for this goal [70]. More recently, PFA (Pulsed Field Ablation) has been proposed as an alternative to RFCA for atrial fibrillation ablation [71,72] since it causes nonthermal myocardial cell death.

Few computational models have been developed for these other energies compared to those for RFCA. Computer modeling has been used to study the temperature distributions in the myocardium during the freeze-thaw cycles during cryoablation [73–75]. Although these models use the same equation to solve the thermal problem as the RFCA models (see Eq. (2) in Section 3.1), they do not solve the electrical problem associated with RF. They also take into account how the properties of the myocardium and the refrigerant change during the phase changes associated with each freeze-thaw cycle.

3. Implementation

3.1. Simplification of the real situation and definition of the model geometry

The first step in the construction of a computational model is the definition of the geometry, which is always a simplification of the real clinical situation. RFCA models typically ignore myocardial surface irregularities and consider the tissue to be smooth. The computational domain, i.e. the surface (in the case of 2D models) or the volume (in 3D models) where the equations will be solved, does not necessarily have to consider the patient's full torso. In fact, it is important to determine any symmetries. For instance, a model similar to that in Fig. 4A, which does not include the problem of fluid dynamics in the blood would present axial symmetry around the catheter axis and hence 2D would be possible. The model in Fig. 4B has plane of symmetry that would cut the catheter and the tissue into two identical halves, so that the computational domain would be reduced to half the real scenario, and the model in Fig. 5 has two planes of symmetry, so that the computational domain would be reduced to a quarter of the real scenario. In other cases, such as those with a more or less realistic full torso (Fig. 6), there are no symmetries and the computational domain coincides with the physical torso.

3.2. Governing equations

All the theoretical models developed for RFCA can be considered mathematical models since they use equations relating to physical variables. First, the electric problem is solved using Laplace's Law:

$$\nabla \cdot (\sigma \nabla \phi) = 0 \tag{1}$$

where σ is the electrical conductivity (S/m) and ϕ the electrical potential (V). RFCA modeling assumes that the tissue has no internal sources, but RF current is generated by imposing boundary conditions on the electrodes or on the outer boundaries of the model. Eq. (1) is solved in the entire model domain (electrodes and tissues) together with the electrical boundary conditions presented in the Appendix. The magnitude of the vector electric field $\boldsymbol{E}$ (V/m) is obtained from $\boldsymbol{E} = -\nabla\phi$, while that the vector of current density $\boldsymbol{J}$ (A/m^2) is calculated from the vector form of Ohm Law, $\boldsymbol{J}=\sigma\cdot\boldsymbol{E}$. The displacement current is considered negligible since σ is much greater than $2\pi f\cdot\varepsilon$, f being the RF frequency (∼500 kHz) and ε the tissue permittivity (F/m). Since a quasi-static approximation is employed for the electrical problem, the electrical variables computed are really DC (direct-current) values which correspond with the root mean squared (RMS) values of the applied RF voltage.

The Bioheat Equation proposed by Pennes [76] has been traditionally used to describe the thermal energy balance in the tissue during RFCA modeling:

$$\rho c \frac{\partial T}{\partial t} = \nabla \cdot (k \cdot \nabla T) - Q_p + Q_m + Q_{RF} \tag{2}$$

where ρ is density (kg/m^3), c specific heat (J/kg·K), T temperature (°C), t time (s), k thermal conductivity (W/m·K), Q_{RF} the heat source caused by RF power (W/m^3), Q_p the heat loss caused by blood perfusion (W/m^3) and Q_m the metabolic heat generation (W/m^3). This last term is ignored for being negligible compared

to the rest of the terms [1], while Q_p (when is considered) is computed as follows:

$$Q_p = \rho_b c_b \omega (T - T_b) \tag{3}$$

where ρ_b is blood density, c_b blood specific heat, T_b body temperature (37 °C), and ω blood perfusion coefficient (at temperature T_b). It must be pointed that other models based on the porous medium theory have also been proposed to model the thermal effect of blood perfusion during RFCA [77,78]. Eq. (2) has been modified in some models using the enthalpy method in order to incorporate the latency heat due to the phase change when the tissue temperature reaches 100 °C [31,32].

After computing temperature progress for each point in the tissue, it is possible to predict the degree of thermal damage and hence to estimate the lesion size induced by RFCA. Like other ablation models, RFCA computer models often use the damage index Ω or the 50 °C isothermal contour [79]. The isotherm has frequently been used in RFCA modeling [12,13,15,16,20–22,33,34,46,51] since it is accepted that the isotherm of irreversible myocardial injury with hyperthermic ablation is likely to be between 50 °C and 56 °C [80]. In contrast, other modeling studies have used the damage index Ω [8,56,62], which models the tissue damage as an irreversible first-order chemical reaction with the rate constant following the Arrhenius relationship [79]:

$$\Omega(t) = \ln\left\{\frac{c(0)}{c(t)}\right\} = \int_0^t A e^{\frac{-\Delta E_a}{RT(\tau)}} d\tau \tag{4}$$

where A is the frequency factor (s^{-1}), ΔE_a is the activation energy for the irreversible damage reaction (J/mol), and R is the universal gas constant (8.314 J/mol·K). In theory a value of $\Omega = 4.6$ is equivalent to 99% cell death probability, while a value of $\Omega = 1$ is equivalent to 63% (both have been used to determine the contour of the lesion). The drawback to this method is that the values of parameters A and ΔE_a are dependent on the tissue type and to date there are no conclusive data for cardiac tissue. Although this is an important limitation, the use of the isotherm does not allow, e.g. assessing lesion growth when RF power has been turned off [44] or when consecutive applications of RF power are made in the same area [56]. In these cases, the use of the method damage index Ω (or any metric that considers temperature and exposure time) is mandatory. In this context, the modeling study by Lau et al. [54] deserves to be highlighted. These authors compared experimental and computational results by different methods of assessing thermal damage: isotherms of 50 °C and 60 °C, the "cumulative equivalent minutes at 43 °C" criterion (less frequently used [32]) and the Arrhenius damage function (Ω=1), finding that the 60 °C contour closely agrees with the *in vitro* lesion measurement of tissue discoloration (as also reported in [13]) while the 50 °C contour matches the other electrophysiological changes related to tissue death, such as loss of excitability [80].

3.3. Tissue properties

The most relevant characteristics of the tissues to consider are density (ρ), specific heat (c), thermal conductivity (k) and electrical conductivity (σ). As the myocardium temperature rises during RFCA its electrical conductivity increases, in the same way as electrolyte solutions and means the electrical impedance gradually drops. It is a process with a huge impact on the process as it works as a positive feedback: the higher the temperature the more conductive the tissue the more RF power is deposited and the greater the heating. For this reason most computational models have included the temperature dependence of σ using variations between 1.2 and 2%/ °C [8,14,16,20,21,28,32,46,53,81]. However, once tissue temperature reaches ~100 °C, tissue dehydration is usually modeled by a sharp drop in sigma of around 2 or 4 orders of magnitude [32,53,82]. Although a specific mathematical model for the dynamics of intramural gas formation has not yet been developed, this approach seems reasonable as the desiccated tissue loses its ability to conduct RF current. However, perhaps in this new state of desiccated tissue the displacement electric current should not be ignored. This method of modeling σ changes with temperature considers reversible changes in tissue properties only (i.e. those not affected by coagulative necrosis). However, as both reversible and irreversible changes actually occur, they could be included in future models, for example by modulating the electrical conductivity with the Arrhenius damage index, as proposed in [83] for RF tumor ablation.

The thermal dependence of k has been also considered in a few models, assuming a linear increment with a coefficient of ~0.0012 $W/m^2 \cdot K \cdot$ °C [21,28,32,82]. This variation is debatable, since some considered to be negative instead of positive [33,81]. The effect of changing the baseline values of c, σ and k has also been studied with variations of ±50% and +100% [16,19]. An interesting review of the temperature dependence of various tissue properties can be found in [84], while the values of different tissue properties can be easily accessed in the ITIS tissue properties database [41].

3.4. Initial and boundary conditions

Initial and boundary conditions must be imposed to provide specific solutions adapted to the specific circumstances to be modeled. It is usual to impose a Dirichlet condition on the active electrode for the electrical problem, specifically a voltage $\phi = V_E$ which corresponds to the RMS value of the RF voltage. A null voltage ($\phi = 0$) is also imposed to model the dispersive electrode, either in the area where this electrode is physically located, in full torso models [11,45] or on the model boundaries when only one area around the active electrode is considered (in these cases the external dimensions must be large enough for the condition not to alter the solution) [11]. These two conditions allow obtaining a unique solution for Eq. (1). Other specific boundary conditions may also be required on symmetry axes or planes. By changing V_E values, different ways of delivering RFCA power can be modeled. The main modes are constant power and constant temperature [21]. To model a constant temperature protocol, the V_E value is modulated during ablation to keep the temperature at a point on the active electrode (where the temperature sensor is assumed to be [16]) around a target value using a control algorithm [47]. In the constant power protocol, V_E is also modulated to keep the power P ($=V_E^2/Z$) around a programmed value, which considers impedance Z to vary throughout the ablation.

For the thermal problem, it is usual to impose Dirichlet conditions on the outer limits of the model, specifically a temperature of $T = 37$ °C, which assumes that these limits are far enough away from the ablation site and therefore keep the body temperature constant. Specific thermal boundary conditions may also be required on the planes or axes of symmetry. All the thermal boundary conditions, together with the initial condition $T = 37$ °C, allow obtaining a unique solution for Eq. (2). The thermal effect of circulating blood is very important in this context and most models have included it in different ways [82]. The most sophisticated of these involves solving fluid dynamics, i.e. obtaining the blood velocity distribution [22], and coupling the solution to Eq. (2) by adding an advection term [83]. In contrast, the simplest way is not to solve the thermal problem in the blood subdomain but only the electrical problem, and to impose boundary conditions that simulate forced convection at the blood-tissue and blood-electrode interfaces. Although this method predicts a lesion depth similar to the method that includes fluid dynamics, it slightly overestimates the surface width and does not provide information on the tem-

perature in the blood, which is important in terms of assessing the risk of thrombi formation. Including the fluid dynamics problem also allows saline infusion to be modeled realistically in irrigated-tip catheters [31–33,81]. Otherwise, the simple way is to impose a fixed temperature on a specific area of the electrode to model the cooling produced by saline as it passes through the electrode [85].

3.5. Computational solvers

Most of the models are solved by numerical techniques because their equations are impossible to solve analytically, either because of the complex model geometry of different types of tissues and materials, or some variables are coupled and this implies non-linear equations. Numerical techniques can include a high degree of complexity both in the geometries and in the relationship between variables and they are always solved using computer software. Most numerical models are built and solved using the Finite Element Method (FEM) which means that the governing equations are solved on a discretized geometry based on a mesh. Linte et al. [86] developed an interesting model which was unlike the traditional FEM models and was solved and implemented using an image-based approach, in which the computational elements were really the image voxels instead of the traditional meshing elements. This was the first attempt to develop a first subject-specific model since the model geometry was based on pre-acquired anatomical three-dimensional (3D) images which were later segmented into blood and tissue compartments. Finally, it should be mentioned that very few analytic studies have been used, possibly due to their comprising a simple geometry based on an oversimplified physical situation [7,42,87].

Despite the availability of an ever-greater number of computational resources, computational models should in general be as simple as possible in order to provide a credible answer to the proposed scientific question. Each computer model simplifies the physical situation in a different way depending on the goal/context of the study. The conclusions must therefore be interpreted by taking the limitations into account. It makes no sense to require that every new computer modeling study includes absolutely every feature suggested to date or every detail imaginable. The modeling expert must have sufficient knowledge of the physics associated with RFCA to decide how to simplify/ignore irrelevant aspects and build the simplest model that allows him/her to study a particular question. There are examples of modeling studies whose objective is to demonstrate that some physical phenomena have very little impact on the result and that they can therefore be ignored in future modeling studies, e.g. the pulsatility associated with circulating blood in the cardiac chamber [88]. Looking for simplicity, some studies aimed to compare different ways of modeling several features, such as the thermal effect of circulating blood [82,85] and thermal lesion size [89].

3.6. Lumped element models

Most of the models (solved both analytically and numerically) considered a continuum physical domain among all the constituent materials (plastic, metal and biological tissue). This type of model is known in engineering as a 'distributed element model', as its attributes (e.g. electrical and thermal conductivities) are distributed evenly throughout the materials (see Fig. 7A). In contrast, the 'lumped element models', which are also widely used in engineering, assume that the attributes are lumped in the domain. These models are not really used in computational modeling RFCA studies since they only reflect the electrical problem. The benefits of lumped element models consist of their simplicity and usefulness for making it easy to understand the electrical problem. In fact, they have only been used by clinical researchers to provide a physical explanation for their experimental results in terms of electrical impedance and the power deposited in the myocardium, blood and torso.

The most frequently proposed lumped element RFCA model considered the blood around the electrode as a resistance R_B in parallel with the resistance associated with the myocardium R_T, and both resistances in series with that representing the rest of the torso tissues until reaching the dispersive electrode, i.e. R_{BODY} [90] (see Fig. 7B). The association of the three resistors determines the electrical impedance recorded before and during RFCA by the RF generator. In this way, the model reflects that the RF current flows from the active electrode taking two parallel paths (R_B and R_T) and that the weight of each of these two resistances has to do with the electrical characteristics of each tissue (e.g. blood is more conductive than myocardium, and hence R_B tends to be smaller than R_T) and the contact surface of the electrode with each element, myocardium or blood (e.g. the deeper the insertion depth of the electrode, the more contact with the myocardium and less with the blood, and therefore R_B tends to be larger than in the case of shallow insertion depth). From the lumped element electrical model, it can be stated that lesion size will be related to the power deposited in the myocardium, i.e. $R_T \cdot I_T^2$, I_T being the part of the total current I that flows exclusively through the myocardium, i.e. $I \cdot R_B/(R_B + R_T)$. The power dissipated in R_T, related to lesion size, can also be estimated by assuming different conditions of applied voltage and catheter angle [91]. Lumped element models have also been used to explain the experimental results of the relationship between baseline impedance, R_{BODY} and lesion size [92].

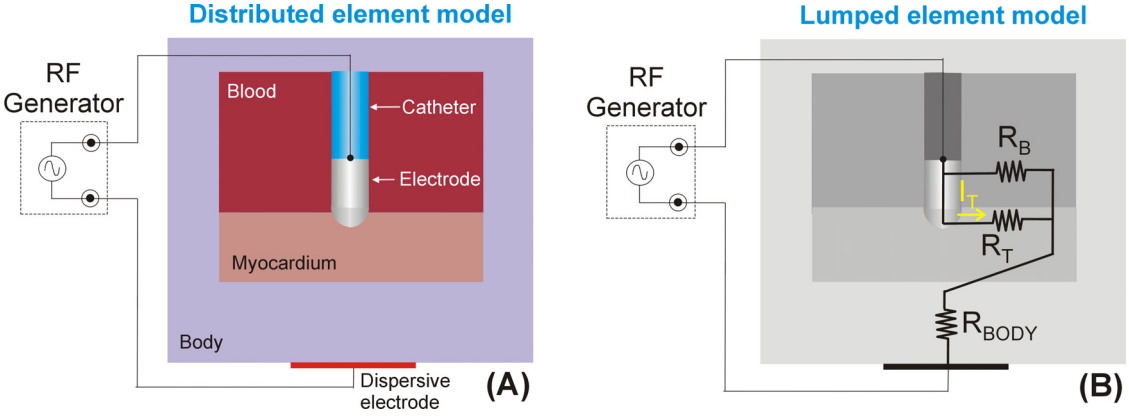

Fig. 7. A: Distributed element RFCA model. **B**: Lumped element RFCA model.

4. Verification and validation

We should not finish this review without paying attention to the verification and validation of computer models. These two concepts are related to questions that any electrophysiologist could/should raise: how reliable is a result obtained from a computer simulation? To what extent can the predictions made by a computer model be used as a reliable basis for clinical decisions [93]? These issues are becoming increasingly relevant, not only because studies based on computer modeling must have the maximum scientific rigor, but because the regulatory agencies of medical devices have recently started receiving and accepting evidence obtained in this way [94,95]. The clinical evaluation of a medical device is a complex and demanding process that aims to obtain sufficient evidence on its efficacy and safety using relevant clinical data from a wide variety of sources. In this regard, computer results would complement data from experiments and clinical studies/trials.

Fig. 8 shows the pipeline of the main steps to build, solve, verify and validate a computational model for RFCA. In any theoretical model the first question is the set of mathematical equations used to reproduce the physics, i.e. the mathematical model. These equations must be supported by physical laws. Laplace's Law is used for the electrical problem, while Navier–Stokes equations (which are based on laws of conservation of momentum and mass for Newtonian fluids) are used when the fluid dynamics associated with circulating blood is considered. The thermal problem is commonly solved by the Bioheat Equation proposed by Pennes [76], which includes a specific term to model the rate of heat transfer between blood and tissue, i.e. the heat losses caused by blood perfusion.

The second question is the data used to build the mathematical model, e.g. the values and ranges of the properties of biological tissues (usually taken from data bases, e.g. the ITIS Foundation [41] and IFAC-CNR [96]). Although in the past some modeling studies conducted sensitivity analyses to assess how results changed with variations of up to ±50% in tissue properties [16], it would be enough to consider the dispersion in tissue properties reported in experimental studies and the range of dimensions of the different tissues involved (e.g. from anatomical studies and imaging techniques).

The third question deals with discretization, which is inherent to any mathematical model solved by a computer. The problem arises from the fact of having to transform the mathematical model into a finite number of discrete components. This is especially relevant in those models that are solved by numerical methods in which the spatial domain (i.e. tissues and catheter) is divided into very small size elements (areas in 2D models and volumes in 3D models; e.g. see Fig. 5B). The governing equations are then solved separately at specific points (nodes) of each element, along with relevant boundary conditions (see e.g. Appendix), thus achieving a continuous solution through the adjacent elements. The size of these elements (called mesh size or size grid) should be smaller in those areas where a large gradient of the variables is expected, which in RFCA is in the surroundings of the active electrode. As a general rule, a mesh size of one tenth of the electrode radius is usually sufficient for RFCA models in which the electrode is considered to be a solid volume [8], but not when considering the specific geometry of the infusion holes when irrigated-tip catheters are modeled, as in [33,81].

In addition, since RFCA is a transitory process, temporal discretization must also be taken into account, i.e. the equations have to be solved step by step. So, the time-step should be smaller at those moments in which the variables change faster. For example, the time step will be shorter during RF application and longer during the post-RF period, in which the tissue cools slowly. In practical terms, keeping the discretization error under control consists of carrying out a convergence test in which the mesh size or the time-step are progressively reduced until consecutive results differ very little. The small difference is the discretization error. The concept of discretization is closely related to the verification of the model. However, the verification must also ensure that the code implementing the computational model represents the mathematical model with sufficient accuracy [93]. In this regard, most RFCA computer models use commercial software whose code has been

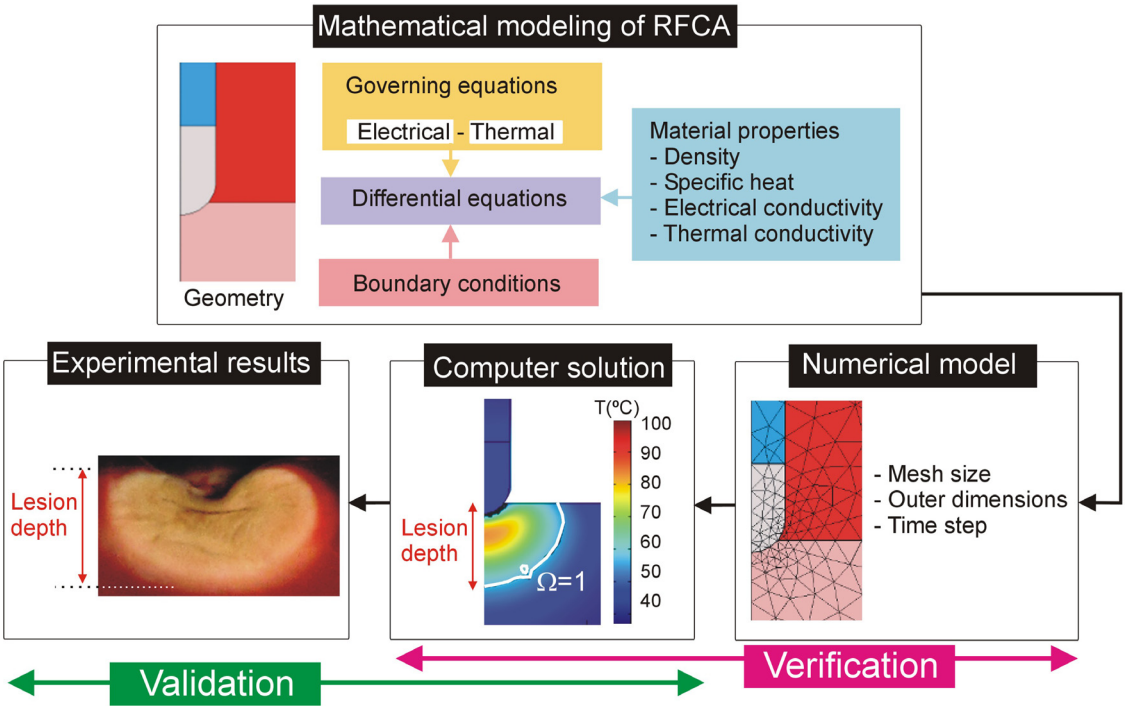

Fig. 8. Pipeline of the main steps to build, solve, verify and validate a computational model for RFCA.

verified by the manufacturer for most of the physical problems included in the model or open-source code verified by the scientific community.

On the other hand, validation implies determining whether the mathematical model represents the actual physical phenomenon with sufficient accuracy [94], i.e. determining the correctness of the underlying assumptions (model geometry, materials properties, boundary conditions and governing equations). In practical terms, this necessarily implies making a comparison between the data provided by the computational model and those obtained from experiments. This comparison must take into account both the uncertainties of the computational model itself and the uncertainties of the experimental method and the data generated [94]. Researchers involved in developing RFCA computational models should conduct uncertainty and sensitivity analyses to assess the model's predictive value using well known techniques such as Latin Hypercube Sampling and Monte Carlo methods [97].

Verification and validation are therefore independent processes. While validation has more to do with the mathematical framework used to represent physical phenomena, verification is related to the implementation of the mathematical model through a code running on a computer. The route map for theoretical models should therefore be: (1) propose a mathematical model (i.e. set of equations and material characteristics), (2) verify the computer model in order to keep the discretization error quantified and controlled, and (3) validate the theoretical model by comparing computer vs. experimental results (taking into account the uncertainties of both the computational model and the experimental method used). A failed validation (i.e. unacceptable discrepancies between computational and experimental results) suggests that some piece of the mathematical model should be modified, since it is assumed that the model has already been verified.

The experimental validation of the theoretical models developed for RFCA has generally been done using experimental data provided by bench-tests based on *ex vivo* models [7,13,15,22,23,33,49,51,54,86]) or phantoms based on tissue-equivalent material (e.g. agar) [8,98–101]. Non-human tissues, e.g. porcine, are almost always used in *ex vivo* experiments. This is relevant since the characteristics of these tissues could differ from those of the human tissues to be ablated in the clinical practice (atrium and ventricle). In fact, Petras et al. [81] carried out a computational study to compare lesion sizes in human and porcine tissues and found different lesion morphologies for the different tissue types and size differences of up to 1 mm.

In vivo or clinical studies are rarely used for validation purpose because both cost and complexity are too high since many variables need to be characterized, such as tissue properties and blood flow at the target site. It is also difficult to obtain information on lesion size and temperature. Unlike clinical studies, the tissue-equivalent material can maintain highly reproducible conditions and situate temperature sensors in precise locations at acceptable levels of cost and complexity [98–100]. *Ex vivo* fragments are also often used, since they reproduce the phenomena associated with temperatures (e.g. steam pops) above which materials like agar melt. Regarding data for validation, several variables have been considered to compare experimental and computational results, such as lesion size in the case of *ex vivo* models [13,15,33,49,51], the progress of the temperature measured in specific points of the ablated sample using very small sensors [22,23,54,85,98–100], infrared thermal imaging [8,101] and the evolution of the electrical variables registered by the RF generator (mainly impedance).

The state of the art shows mathematical and computer models capable of predicting reasonably well the shape and size of lesions under specific conditions. Most mathematical models performed well from a qualitative point of view (even though they reported prediction errors of up to 100% [51]), i.e. they showed the same behavior as the experimental models when certain parameters were changed (e.g. power, duration, blood flow) [13,15,49]. In quantitative terms, most computer models predict the tissue temperature at depth > 3 mm [23] quite well, with errors $< 3 - 7$ °C [8,22,5,86,100]. The studies have reported prediction errors of lesion sizes of from 1 mm [31,86] to 2 mm [31], with a tendency to better predict depth than width (surface and maximum). A recent meticulous study by Rossman et al. [101] on phantom agar even reported slightly minor errors ($0.1 - 0.7$ mm for lesion width and $0.3 - 0.7$ mm for lesion depth). Despite the fact that prediction errors of up to ~50% have been reported for the maximum width, the computed depths and widths have been within the range of the corresponding experimental values [33]. Prediction errors are often associated with the uncertainty in the method of identifying the lesion contour (areas of discoloration in *ex vivo* models vs. mathematical models of thermal damage) and the spatial position of temperature sensors. Once more, it should be emphasized that some phenomena associated with very high temperatures (such as the formation of steam pops, charring, etc.) are not yet fully understood from the physical point of view, so there is no mathematical framework that describes them and therefore they have not yet been able to be reliably incorporated into computational models.

5. Current limitations and future work

5.1. What still remains to be modeled

Many details of RFCA biophysics still remain to be modeled from a mathematical/ theoretical point of view. One of the most urgent issues is to achieve a mathematical framework able to describe the occurrence of intramural steam pops, their relationship to rises in impedance and the risk of their disrupting the endocardial surface. To date, computer models have associated the steam pop phenomenon with tissue temperatures around 100 °C. However, it seems reasonable to suspect that the creation of intra-tissue steam should not always be associated with an audible pop or a sudden rise in impedance since the gas could diffuse to the tissue surface [102]. Future work should therefore be directed towards building a model able to include the formation and movement of steam within the tissue, along the same lines as that proposed by Zhu et al. [103] for RF tumor ablation, and, although rare, RFCA can even lead to wall perforation [104]. Even though no computer model can yet describe this complication, it could be based on the model proposed by Shimko et al. [105] to study temperature distributions during RF-induced perforation of atrial septal defects in newborns. These authors solved the model by the Finite Difference Method (DFM) and assumed that the tissue elements in contact with the electrode over 100 °C were instantly vaporized, so that the electrode advanced one step forward over them.

In modeling irrigated-tip catheters, saline irrigation has been taken into account to date by an inlet velocity condition into the blood region, either applied in a specific zone of the electrode surface where the irrigation holes are expected to be situated [31,32] or directly at the holes modeled [33,81]. In any case, this is only an approximation which assumes that blood and saline mix perfectly so that the electrical and thermal characteristics of the saline do not affect the blood surrounding the electrode. Improved future models built on the basis of mixture theory could be considered to model, for instance, RFCA with irrigated electrodes in which the electrical conductivity of the saline is half reduced [106]. Likewise, computational modeling of interstitial infusion electrodes for RFCA (i.e. needle-tip electrodes which inject warm saline into the tissue [107]), will require adding a mathematical framework that takes into account how heated saline diffuses into tissue and how it alters electrical and thermal conditions, for example using the hydraulic conductivity model based on Darcy's Law [108].

Although experimental data on the electrical [109] and thermal [110] characteristics of cardiac tissue are available, there is not yet a full characterization of the irreversible changes associated with heating as has already been done for other tissues [111–113], and the information on thermal conductivity of cardiac tissue after heating is very limited [114]. This information will be crucial in future computer modeling studies to assess the effect of overlapping lesions, which is usually done by creating continuous linear lesions using a point-to-point technique in the context of atrial fibrillation ablation. There is also a current lack of characterization of the mechanical changes in cardiac tissue when subjected to forces (due to the electrode pressure) or heat-induced shrinkage. In conclusion, all these current limitations suggest that we are still far from making computer modeling a patient-specific predictive tool of lesion size based on pre-ablation medical tests and measurements.

5.2. Future work

The development of theoretical models based mainly on computer simulations in the last 30 years has gone hand in hand with the development of new catheters as well as new ways of ablating the tissue causing cardiac arrhythmias. They have been and will continue to be in the future a complementary technique to experimental and clinical studies. Some models have served to understand the biophysics associated with some of the phenomena that occur during RFCA and to aid in the development of ablative technologies, indirectly contributing to making RFCA safer and more effective.

To date, the computer modeling of RFCA has been developed along two lines of work that unfortunately have rarely converged: one that tries to predict the lesion size (which was the subject of this review) and one that, on the basis of modeling the functioning electrophysiological myocardium, tries to predict why a specific therapy (lesion size and shape) will be successful or not in a given arrhythmogenic substrate [115,116]. In the future these two lines must converge if what is sought is personalized modeling on the basis of integrating physiological data of the target substrate, anatomical conditions of myocardium and adjacent organs, tissue electrical and thermal properties, and highly technical details of the RF catheter, its location and interaction with the target, and the way of creating the thermal lesion. This idea should be equally valid for applicators based on any energy type (microwave, laser, ultrasound, pulsed-field, etc.) capable of treating the arrhythmogenic substrate.

RFCA computer modeling could become a tool in planning treatments. In theory, computer modeling could play the same role as dose planning in body radiation therapy for ventricular tachycardia [117], or the personalized electrophysiological models [118], which are still incipient techniques. In the case of RFCA, the sequence could be as follows: The necessary information to build the model must be acquired previously, including anatomical aspects from a medical image (heart, torso, dispersive electrode position, type of tissues near the ablation site) and technology (type of catheter and electrode, mode of power application). Once the medical procedure has started, the RF electrode can be accurately positioned by the already available navigation systems [119]. Once the RF electrode is on the target, the information needed to build the model can be completed, including the electrical and thermal properties of the substrate (by measurements from the RF electrode itself or other accessory electrodes), electrode-tissue contact (e.g. by impedance measurements [36] and contact force [120]), and cooling capability of the circulating blood in the area of ablation (e.g. by thermal analysis after application of a low power pulse [120,121]). With all this information, the model could predict the lesion size and the maximum temperatures reached in blood, myocardium and nearby tissues. This information prior to ablation would be useful in terms of efficacy and safety.

Second, during the application of RF power, a large amount of information is available from the progress of the impedance, temperature [122] and contact force measured in the RF catheter, besides other strategically placed sensors [123]. Non-invasive techniques such as Electrical Impedance Tomography (EIT) have also been studied to estimate the temperature map in real time during RFCA [124,125], which can be complemented by others to assess subsequent evolution of the lesion size [126]. Finally, as previously mentioned, although *in vivo* and clinical studies are rarely used to validate computational models, the complete development of a modeling-based RFCA planning tool would require a validation of this type.

Funding details

Grant RTI2018-094357-B-C21 funded by MCIN/AEI/10.13039/501100011033 (Spanish Ministerio de Ciencia, Innovación y Universidades/Agencia Estatal de Investigación).

Declaration of Competing Interest

The authors have no conflicts to disclose.

Appendix. Path of RF current through the tissues and the electric boundary conditions

The electrical boundary conditions for electric field described as the electric field vector **E** modifies its direction when crossing an interface between two media with a different electrical conductivity (σ). Fig. 9 illustrates this phenomenon using a computer model which includes a spherical fragment of tissue near the ablation electrode. Two cases are considered, one in which the tissue fragment is less conductive than the myocardium (e.g. fat), and another in which the fragment is more conductive (e.g. the same myocardium heated, since σ increases by ~2%/ °C). Although the explanation is provided in terms of electric field vector **E**, in the case of RFCA the direction of vector **E** can be assumed to be the same as that of current density vector **J**, since displacement current is negligible vs. conductive current [40], so that both vectors are simply related by means of Ohm's Law in vector form, $\boldsymbol{J}=\sigma\cdot\mathbf{E}$. Fig. 9 shows the computed electrical field (**E**) lines (black) and the equipotential lines, which represent the points with equal electric potential or voltage ϕ (white lines, always perpendicular to **E** since $E=-\nabla\phi$). The background color represents the electrical conductivity (σ) of each material (scale in S/m). The metal electrode (the most conductive) is white, the plastic of the catheter (the least conductive) is black, fat is less conductive than myocardium ($\sigma_1<\sigma_2$), and heated myocardium is more conductive than unheated ($\sigma_3>\sigma_2$). Note that while electric field lines (which are related to the path of the RF current through the tissues) tend to bypass fatty tissue (Fig. 9B) but tend to go toward heated tissue (Fig. 9C). Fig. 9A,D graphically explains these tendencies in terms of the two boundary conditions governing the **E** vector at the interface of two zones with different σ values. Condition 1: Tangential component of **E** (E_t) is continuous across the interface (i.e. the tangential value is the same in the two adjoining subregions $E_{t,1}=E_{t,2}$). Condition 2: Normal (i.e. perpendicular) component of **E** (E_n) is not continuous across the interface and is governed by the following equation $\sigma_1\cdot E_{n,1}=\sigma_2\cdot E_{n,2}$. So, Fig. 9D illustrates as saying that the RF current tends towards a more conductive area (heated zone) is equivalent to saying that the normal component is greater ($E_{n,2}$) in the less conductive medium (σ_2). Likewise, Fig. 9A shows that saying that the RF current bypasses a less conductive area (fat) is equivalent

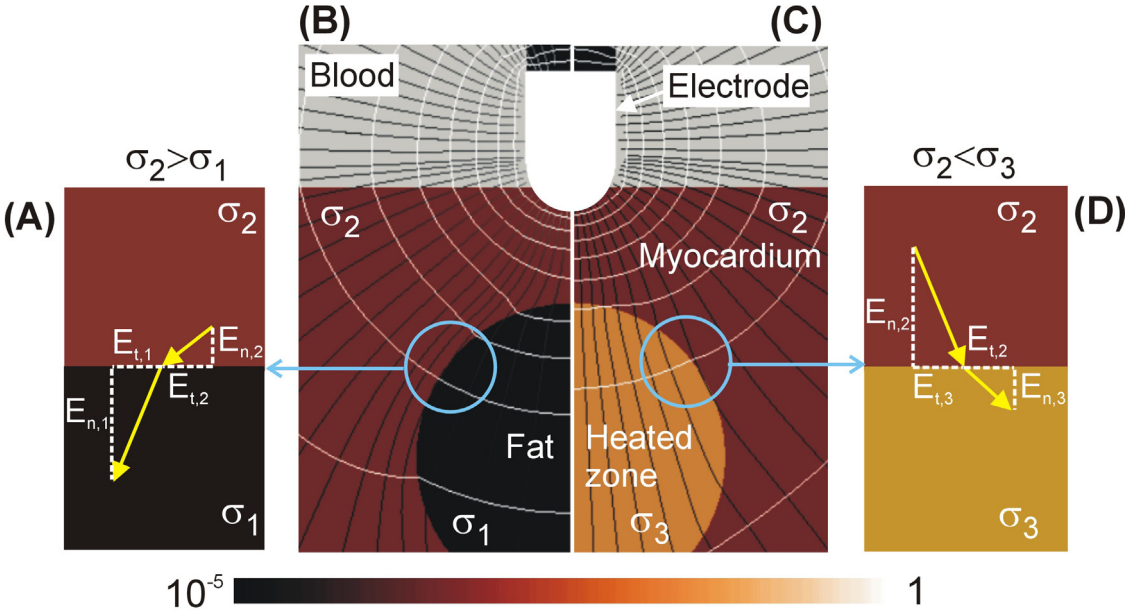

Fig. 9. RFCA computer results showing electrical field (**E**-vector) lines (black) and equipotential (ϕ) lines (white). The background color represents the electrical conductivity (σ) of the different materials (scale in S/m). Two cases are considered, one in which a fragment of poorly conductive tissue (e.g. fat) is included near the electrode tip (**B**), and another in which the fragment is more conductive than the myocardium, e.g. the same myocardium heated (**C**). **A, D:** Graphical explanation of the boundary conditions governing the E vector. [*Results obtained from FEniCS* (https://fenicsproject.org)].

to saying that the normal component is smaller ($E_{n,2}$) in the more conductive medium (σ_2).

References

[1] E.J. Berjano, Theoretical modeling for radiofrequency ablation: state-of-the-art and challenges for the future, Biomed. Eng. Online 5 (2006) 24 Apr 18, doi:10.1186/1475-925X-5-24.

[2] S. Singh, R. Melnik, Thermal ablation of biological tissues in disease treatment: a review of computational models and future directions, Electromagn. Biol. Med. 39 (2) (2020) 49–88, doi:10.1080/15368378.2020.1741383.

[3] B. Avitall, M. Khan, D. Krum, J. Hare, C. Lessila, A. Dhala, S. Deshpande, M. Jazayeri, J. Sra, M. Akhtar, Physics and engineering of transcatheter cardiac tissue ablation, J. Am. Coll. Cardiol. 22 (3) (1993) 921–932, doi:10.1016/0735-1097(93)90212-j.

[4] D. Haines, Biophysics of ablation: application to technology, J. Cardiovasc. Electrophysiol. 15 (10 Suppl) (2004) S2–S11, doi:10.1046/j.1540-8167.2004.15102.x.

[5] F.H. Wittkampf, H. Nakagawa, RF catheter ablation: lessons on lesions, Pacing Clin. Electrophysiol. 29 (11) (2006) 1285–1297, doi:10.1111/j.1540-8159.2006.00533.x.

[6] D.E. Haines, D.D. Watson, Tissue heating during radiofrequency catheter ablation: a thermodynamic model and observations in isolated perfused and superfused canine right ventricular free wall, Pacing Clin. Electrophysiol. 12 (6) (1989) 962–976, doi:10.1111/j.1540-8159.1989.tb05034.x.

[7] D.E. Haines, D.D. Watson, A.F. Verow, Electrode radius predicts lesion radius during radiofrequency energy heating. Validation of a proposed thermodynamic model, Circ. Res. 67 (1) (1990) 124–129, doi:10.1161/01.res.67.1.124.

[8] S. Labonté, Numerical model for radio-frequency ablation of the endocardium and its experimental validation, IEEE Trans. Biomed. Eng. 41 (2) (1994) 108–115, doi:10.1109/10.284921.

[9] S. Labonté, A computer simulation of radio-frequency ablation of the endocardium, IEEE Trans. Biomed. Eng. 41 (9) (1994) 883–890, doi:10.1109/10.312096.

[10] L.T. Blouin, F.I. Marcus, L. Lampe, Assessment of effects of a radiofrequency energy field and thermistor location in an electrode catheter on the accuracy of temperature measurement, Pacing Clin. Electrophysiol. 14 (5 Pt 1) (1991) 807–813, doi:10.1111/j.1540-8159.1991.tb04111.x.

[11] A.V. Shahidi, P. Savard, A finite element model for radiofrequency ablation of the myocardium, IEEE Trans. Biomed. Eng. 41 (10) (1994) 963–968, doi:10.1109/10.324528.

[12] Z. Kaouk, A. Vahid Shahidi, P. Savard, F. Molin, Modelling of myocardial temperature distribution during radio-frequency ablation, Med. Biol. Eng. Comput. 34 (2) (1996) 165–170, doi:10.1007/BF02520023.

[13] D. Panescu, J.G. Whayne, S.D. Fleischman, M.S. Mirotznik, D.K. Swanson, J.G. Webster, Three-dimensional finite element analysis of current density and temperature distributions during radio-frequency ablation, IEEE Trans. Biomed. Eng. 42 (9) (1995) 879–890, doi:10.1109/10.412649.

[14] S. Tungjitkusolmun, E.J. Woo, H. Cao, J.Z. Tsai, V.R. Vorperian, J.G. Webster, Finite element analyses of uniform current density electrodes for radiofrequency cardiac ablation, IEEE Trans. Biomed. Eng. 47 (1) (2000) 32–40, doi:10.1109/10.817617.

[15] E.J. Woo, S. Tungjitkusolmun, H. Cao, J.Z. Tsai, J.G. Webster, V.R. Vorperian, J.A. Will, A new catheter design using needle electrode for subendocardial RF ablation of ventricular muscles: finite element analysis and *in vitro* experiments, IEEE Trans. Biomed. Eng. 47 (1) (2000) 23–31, doi:10.1109/10.817616.

[16] S. Tungjitkusolmun, E.J. Woo, H. Cao, J.Z. Tsai, V.R. Vorperian, J.G. Webster, Thermal–electrical finite element modelling for radio frequency cardiac ablation: effects of changes in myocardial properties, Med. Biol. Eng. Comput. 38 (5) (2000) 562–568, doi:10.1007/BF02345754.

[17] S. Tungjitkusolmun, V.R. Vorperian, N. Bhavaraju, H. Cao, J.Z. Tsai, J.G. Webster, Guidelines for predicting lesion size at common endocardial locations during radio-frequency ablation, IEEE Trans. Biomed. Eng. 48 (2) (2001) 194–201, doi:10.1109/10.909640.

[18] Y.C. Lai, Y.B. Choy, D. Haemmerich, V.R. Vorperian, J.G. Webster, Lesion size estimator of cardiac radiofrequency ablation at different common locations with different tip temperatures, IEEE Trans. Biomed. Eng. 51 (10) (2004) 1859–1864, doi:10.1109/TBME.2004.831529.

[19] S. Tungjitkusolmun, D. Haemmerich, H. Cao, J.Z. Tsai, Y.B. Choy, V.R. Vorperian, J.G. Webster, Modeling bipolar phase-shifted multielectrode catheter ablation, IEEE Trans. Biomed. Eng. 49 (1) (2002) 10–17, doi:10.1109/10.972835.

[20] M.K. Jain, G. Tomassoni, R.E. Riley, P.D. Wolf, Effect of skin electrode location on radiofrequency ablation lesions: an *in vivo* and a three-dimensional finite element study, J. Cardiovasc. Electrophysiol. 9 (12) (1998) 1325–1335, doi:10.1111/j.1540-8167.1998.tb00108.x.

[21] M.K. Jain, P.D. Wolf, Temperature-controlled and constant-power radiofrequency ablation: what affects lesion growth? IEEE Trans. Biomed. Eng. 46 (12) (1999) 1405–1412, doi:10.1109/10.804568.

[22] M.K. Jain, P.D. Wolf, A three-dimensional finite element model of radiofrequency ablation with blood flow and its experimental validation, Ann. Biomed. Eng. 28 (9) (2000) 1075–1084, doi:10.1114/1.1310219.

[23] D. Demazumder, M.S. Mirotznik, D. Schwartzman, Biophysics of radiofrequency ablation using an irrigated electrode, J. Interv. Card. Electrophysiol. 5 (4) (2001) 377–389, doi:10.1023/a:1013224110550.

[24] J.J. Pérez, A. D'Avila, A. Aryana, E. Berjano, Electrical and thermal effects of esophageal temperature probes on radiofrequency catheter ablation of atrial fibrillation: results from a computational modeling study, J. Cardiovasc. Electrophysiol. 26 (5) (2015) 556–564, doi:10.1111/jce.12630.

[25] J.J. Pérez, A. D'Avila, A. Aryana, M. Trujillo, E Berjano, Can fat deposition after myocardial infarction alter the performance of RF catheter ablation of scar-related ventricular tachycardia?: Results from a computer modeling study, J. Cardiovasc. Electrophysiol. 27 (8) (2016) 947–952, doi:10.1111/jce.13006.

[26] J.J. Pérez, A. González-Suárez, E. Berjano, Numerical analysis of thermal impact of intramyocardial capillary blood flow during radiofrequency cardiac ablation, Int. J. Hyperth. 34 (3) (2018) 243–249, doi:10.1080/02656736.2017.1336258.

[27] J.M. Guerra, E. Jorge, S. Raga, C. Gálvez-Montón, C. Alonso-Martín, E. Rodríguez-Font, J. Cinca, X. Viñolas, Effects of open-irrigated radiofrequency ablation catheter design on lesion formation and complications: *in vitro* comparison of 6 different devices, J. Cardiovasc. Electrophysiol. 24 (10) (2013) 1157–1162, doi:10.1111/jce.12175.

[28] E.J. Berjano, F. Hornero, What affects esophageal injury during radiofrequency ablation of the left atrium? An engineering study based on finite-element analysis, Physiol. Meas. 26 (5) (2005) 837–848, doi:10.1088/0967-3334/26/5/020.

[29] E.J. Berjano, F. Hornero, A cooled intraesophageal balloon to prevent thermal injury during endocardial surgical radiofrequency ablation of the left atrium: a finite element study, Phys. Med. Biol. 50 (20) (2005) N269–N279, doi:10.1088/0031-9155/50/20/N03.

[30] F. Hornero, E.J. Berjano, Esophageal temperature during radiofrequency-catheter ablation of left atrium: a three-dimensional computer modeling study, J. Cardiovasc. Electrophysiol. 17 (4) (2006) 405–410, doi:10.1111/j.1540-8167.2006.00404.x.

[31] A. González-Suárez, E. Berjano, J.M. Guerra, L. Gerardo-Giorda, Computational modeling of open-irrigated electrodes for radiofrequency cardiac ablation including blood motion-saline flow interaction, PLoS ONE 11 (3) (2016) e0150356, doi:10.1371/journal.pone.0150356.

[32] H. Avari, C. Berkmortel, E. Savory, An insight to the role of thermal effects on the onset of atrioesophageal fistula: a computer model of open-irrigated radiofrequency ablation, Cardiovasc. Eng. Technol. 11 (4) (2020) 481–493, doi:10.1007/s13239-020-00465-z.

[33] A. Petras, M. Leoni, J.M. Guerra, J. Jansson, L. Gerardo-Giorda, A computational model of open-irrigated radiofrequency catheter ablation accounting for mechanical properties of the cardiac tissue, Int. J. Numer Method Biomed. Eng. 35 (11) (2019) e3232, doi:10.1002/cnm.3232.

[34] S. Singh, R. Melnik, Computational modeling of cardiac ablation incorporating electrothermomechanical interactions, ASME J. Med. Diagn. 3 (4) (2020), doi:10.1115/1.4048536.

[35] S. Yan, K. Gu, X. Wu, W. Wang, Computer simulation study on the effect of electrode-tissue contact force on thermal lesion size in cardiac radiofrequency ablation, Int. J. Hyperth. 37 (1) (2020) 37–48, doi:10.1080/02656736.2019.1708482.

[36] H. Cao, M.A. Speidel, J.Z. Tsai, M.S. Van Lysel, V.R. Vorperian, J.G. Webster, FEM analysis of predicting electrode-myocardium contact from RF cardiac catheter ablation system impedance, IEEE Trans. Biomed. Eng. 49 (6) (2002) 520–526, doi:10.1109/TBME.2002.1001965.

[37] F. Wittkampf, H. Nakagawa, Short high-power RF application, J. Cardiovasc. Electrophysiol. 29 (2) (2018) 328–329, doi:10.1111/jce.13392.

[38] I.D. McRury, D. Panescu, M.A. Mitchell, D.E. Haines, Nonuniform heating during radiofrequency catheter ablation with long electrodes: monitoring the edge effect, Circulation 96 (11) (1997) 4057–4064, doi:10.1161/01.cir.96.11.4057.

[39] J.S. Koruth, V.Y. Reddy, M.A. Miller, K.K. Patel, J.O. Coffey, A. Fischer, J.A. Gomes, S. Dukkipati, A. D'Avila, A. Mittnacht, Mechanical esophageal displacement during catheter ablation for atrial fibrillation, J. Cardiovasc. Electrophysiol. 23 (2) (2012) 147–154, doi:10.1111/j.1540-8167.2011.02162.x.

[40] J.A. Pearce, Electrosurgery, Electrosurgery, Chapman and Hall, 1986.

[41] Hasgall P.A., Di Gennaro F., Baumgartner C., Neufeld E., Gosselin M.C., Payne D., Klingenböck A., Kuster N.: IT'IS Database for thermal and electromagnetic parameters of biological tissues, Version 3.0, September 01st, 2015, Doi: 10.13099/VIP21000-03-0. www.itis.ethz.ch/database.

[42] L. Consiglieri, An analytical solution for a bio-heat transfer problem, Int. J. Bio-Sci. Bio-Technol. 5 (2013) 267–278.

[43] F.H. Wittkampf, H. Nakagawa, W.S. Yamanashi, S. Imai, W.M. Jackman, Thermal latency in radiofrequency ablation, Circulation 93 (6) (1996) 1083–1086, doi:10.1161/01.cir.93.6.1083.

[44] R.M. Irastorza, A. d'Avila, E. Berjano, Thermal latency adds to lesion depth after application of high-power short-duration radiofrequency energy: results of a computer-modeling study, J. Cardiovasc. Electrophysiol. 29 (2) (2018) 322–327, doi:10.1111/jce.13363.

[45] R.M. Irastorza, A. Gonzalez-Suarez, J.J. Pérez, E. Berjano, Differences in applied electrical power between full thorax models and limited-domain models for RF cardiac ablation, Int. J. Hyperth. 37 (1) (2020) 677–687, doi:10.1080/02656736.2020.1777330.

[46] D. Schutt, E.J. Berjano, D. Haemmerich, Effect of electrode thermal conductivity in cardiac radiofrequency catheter ablation: a computational modeling study, Int. J. Hyperth. 25 (2) (2009) 99–107, doi:10.1080/02656730802563051.

[47] J. Alba-Martínez, M. Trujillo, R. Blasco-Giménez, E. Berjano, Could it be advantageous to tune the temperature controller during radiofrequency ablation? A feasibility study using theoretical models, Int. J. Hyperth. 27 (6) (2011) 539–548, doi:10.3109/02656736.2011.586665.

[48] S. Coderch-Navarro, E. Berjano, O. Camara, A. González-Suárez, High-power short-duration vs. standard radiofrequency cardiac ablation: comparative study based on an in-silico model, Int. J. Hyperth. 38 (1) (2021) 582–592, doi:10.1080/02656736.2021.1909148.

[49] F. Bourier, J. Duchateau, K. Vlachos, A. Lam, C.A. Martin, M. Takigawa, T. Kitamura, A. Frontera, G. Cheniti, T. Pambrun, N. Klotz, A. Denis, N. Derval, H. Cochet, F. Sacher, M. Hocini, M. Haïssaguerre, P. Jais, High-power short-duration versus standard radiofrequency ablation: insights on lesion metrics, J. Cardiovasc. Electrophysiol. 29 (11) (2018) 1570–1575, doi:10.1111/jce.13724.

[50] F. Bourier, K. Vlachos, A. Frontera, C.A. Martin, A. Lam, M. Takigawa, T. Kitamura, G. Cheniti, J. Duchateau, T. Pambrun, N. Derval, A. Denis, H. Cochet, M. Hocini, F. Sacher, M. Haïssaguerre, P. Jaïs, In silico analysis of the relation between conventional and high-power short-duration RF ablation settings and resulting lesion metrics, J. Cardiovasc. Electrophysiol. 31 (6) (2020) 1332–1339, doi:10.1111/jce.14495.

[51] S. Yan, X. Wu, W. Wang, Theoretical and experimental analysis of amplitude control ablation and bipolar ablation in creating linear lesion and discrete lesions for treating atrial fibrillation, Int. J. Hyperth. 33 (6) (2017) 608–616, doi:10.1080/02656736.2017.1286390.

[52] K. Gu, Y. Wang, S. Yan, X Wu, Modeling analysis of thermal lesion characteristics of unipolar/bipolar ablation using circumferential multipolar catheter, Appl. Sci. 10 (2020) 9081, doi:10.3390/app10249081.

[53] S. Yan, X. Wu, W. Wang, A simulation study to compare the phase-shift angle radiofrequency ablation mode with bipolar and unipolar modes in creating linear lesions for atrial fibrillation ablation, Int. J. Hyperth. 32 (3) (2016) 231–238, doi:10.3109/02656736.2016.1145746.

[54] M. Lau, B. Hu, R. Werneth, M. Sherman, H. Oral, F. Morady, P. Krysl, A theoretical and experimental analysis of radiofrequency ablation with a multielectrode, phased, duty-cycled system, Pacing Clin. Electrophysiol. 33 (9) (2010) 1089–1100, doi:10.1111/j.1540-8159.2010.02801.x.

[55] A. González-Suárez, A. d'Avila, J.J. Pérez, V.Y. Reddy, O. Camara, E. Berjano, Thermal impact of balloon occlusion of the coronary sinus during mitral isthmus radiofrequency ablation: an in-silico study, Int. J. Hyperth. 36 (1) (2019) 1168–1177, doi:10.1080/02656736.2019.1686181.

[56] A. González-Suárez, M. Trujillo, J. Koruth, A. d'Avila, E. Berjano, Radiofrequency cardiac ablation with catheters placed on opposing sides of the ventricular wall: computer modelling comparing bipolar and unipolar modes, Int. J. Hyperth. 30 (6) (2014) 372–384, doi:10.3109/02656736.2014.949878.

[57] J. Gopalakrishnan, A mathematical model for irrigated epicardial radiofrequency ablation, Ann. Biomed. Eng. 30 (7) (2002) 884–893, doi:10.1114/1.1507845.

[58] E.J. Berjano, F. Hornero, Thermal-electrical modeling for epicardial atrial radiofrequency ablation, IEEE Trans. Biomed. Eng. 51 (8) (2004) 1348–1357, doi:10.1109/TBME.2004.827545.

[59] A.G. Suárez, F. Hornero, E.J. Berjano, Mathematical modeling of epicardial RF ablation of atrial tissue with overlying epicardial fat, Open Biomed. Eng. J. 4 (2010) 47–55, doi:10.2174/1874120701004020047.

[60] J.J. Pérez, A. González-Suárez, A. d'Avila, E. Berjano, RF-energised intracoronary guidewire to enhance bipolar ablation of the interventricular septum: *in-silico* feasibility study, Int. J. Hyperth. 34 (8) (2018) 1202–1212, doi:10.1080/02656736.2018.1425487.

[61] M.M. Montoya, S. Mickelsen, B. Clark, M. Arnold, J. Hanks, E. Sauter, E. Kulstad, Protecting the esophagus from thermal injury during radiofrequency ablation with an esophageal cooling device, J. Atr. Fibrillation 11 (5) (2019) 2110, doi:10.4022/jafib.2110.

[62] M. Mercado, L. Leung, M. Gallagher, S. Shah, E. Kulstad, Modeling esophageal protection from radiofrequency ablation via a cooling device: an analysis of the effects of ablation power and heart wall dimensions, Biomed. Eng. Online 19 (1) (2020) 77, doi:10.1186/s12938-020-00821-z.

[63] A. González-Suárez, D. Herranz, E. Berjano, J.L. Rubio-Guivernau, E. Margallo-Balbás, Relation between denaturation time measured by optical coherence reflectometry and thermal lesion depth during radiofrequency cardiac ablation: feasibility numerical study, Lasers Surg. Med. 50 (3) (2018) 222–229, doi:10.1002/lsm.22771.

[64] A. Verma, M.M. Schmidt, J.P. Lalonde, D.A. Ramirez, M.K. Getman, Assessing the relationship of applied force and ablation duration on lesion size using a diamond tip catheter ablation system, Circ. Arrhythm. Electrophysiol. (2021), doi:10.1161/CIRCEP.120.009541.

[65] C. Rappaport, Cardiac tissue ablation with catheter-based microwave heating, Int. J. Hyperth. 20 (7) (2004) 769–780, doi:10.1080/02656730412331286885.

[66] H.F. Tse, S. Liao, C.W. Siu, L. Yuan, J. Nicholls, G. Leung, T. Ormsby, G.K. Feld, C.P. Lau, Determinants of lesion dimensions during transcatheter microwave ablation, Pacing Clin. Electrophysiol. 32 (2) (2009) 201–208, doi:10.1111/j.1540-8159.2008.02203.x.

[67] F. Lü, W. Huang, D.G. Benditt, A feasibility study of noninvasive ablation of ventricular tachycardia using high-intensity focused ultrasound, J. Cardiovasc. Electrophysiol. 29 (5) (2018) 788–794, doi:10.1111/jce.13459.

[68] F. Bessiere, W.A. N'djin, E.C. Colas, F. Chavrier, P. Greillier, J.Y. Chapelon, P. Chevalier, C Lafon, Ultrasound-guided transesophageal high-intensity focused ultrasound cardiac ablation in a beating heart: a pilot feasibility study in pigs, Ultrasound Med. Biol. 42 (8) (2016) 1848–1861, doi:10.1016/j.ultrasmedbio.2016.03.007.

[69] M. Yano, Y. Egami, K. Ukita, A. Kawamura, H. Nakamura, Y. Matsuhiro, K. Yasumoto, M. Tsuda, N. Okamoto, Y. Matsunaga-Lee, R. Shutta, M. Nishino, J. Tanouchi, Impact of myocardial injury and inflammation due to ablation on the short-term and mid-term outcomes: cryoballoon versus laser balloon ablation, Int. J. Cardiol. 338 (2021) 102–108, doi:10.1016/j.ijcard.2021.06.016.

[70] K. Nagashima, Y. Okumura, I. Watanabe, S. Nakahara, Y. Hori, K. Iso, R. Watanabe, M. Arai, Y. Wakamatsu, S. Kurokawa, H. Mano, T. Nakai, K. Ohkubo, A. Hirayama, Hot balloon versus cryoballoon ablation for atrial fibrillation: lesion characteristics and middle-term outcomes, Circ. Arrhythm. Electrophysiol. 11 (5) (2018) e005861, doi:10.1161/CIRCEP.117.005861.

[71] L. Di Biase, J.C. Diaz, X.D. Zhang, J. Romero, Pulsed field catheter ablation in atrial fibrillation, Trends Cardiovasc. Med. (2021), doi:10.1016/j.tcm.2021.07.006.

[72] K. Kuroki, W. Whang, C. Eggert, J. Lam, J. Leavitt, I. Kawamura, A. Reddy, B. Morrow, C. Schneider, J. Petru, M.K. Turagam, J.S. Koruth, M.A. Miller, S. Choudry, B. Ellsworth, S.R. Dukkipati, P. Neuzil, V.Y. Reddy, Ostial dimensional changes after pulmonary vein isolation: pulsed field ablation vs radiofrequency ablation, Heart Rhythm. 17 (9) (2020) 1528–1535, doi:10.1016/j.hrthm.2020.04.040.
[73] M.K. Getman, E. Wissner, R. Ranjan, J.P. Lalonde, Relationship between time-to-isolation and freeze duration: computational modeling of dosing for arctic front advance and arctic front advance pro cryoballoons, J. Cardiovasc. Electrophysiol. 30 (11) (2019) 2274–2282, doi:10.1111/jce.14150.
[74] M. Handler, G. Fischer, M. Seger, R. Kienast, F. Hanser, C. Baumgartner, Simulation and evaluation of freeze-thaw cryoablation scenarios for the treatment of cardiac arrhythmias, Biomed. Eng. Online 14 (2015) 12, doi:10.1186/s12938-015-0005-9.
[75] M. Handler, G. Fischer, M. Seger, R. Kienast, C.N. Nowak, D. Pehböck, F. Hintringer, C. Baumgartner, Computer simulation of cardiac cryoablation: comparison with in vivo data, Med. Eng. Phys. 35 (12) (2013) 1754–1761, doi:10.1016/j.medengphy.2013.07.006.
[76] H.H. Pennes, Analysis of tissue and arterial blood temperatures in the resting human forearm, J. Appl. Physiol. 1 (2) (1948) 93–122, doi:10.1152/jappl.1948.1.2.93.
[77] M. Iasiello, A. Andreozzi, N. Bianco, K. Vafai, The porous media theory applied to radiofrequency catheter ablation, Int. J. Numer. Methods Heat Fluid Flow 30 (5) (2020) 2669–2681, doi:10.1108/HFF-11-2018-0707.
[78] S. Singh, R. Melnik, Fluid-structure interaction and non-fourier effects in coupled electro-thermo-mechanical models for cardiac ablation, Fluids 6 (2021) 294, doi:10.3390/fluids6080294.
[79] B.L. Viglianti, M.W. Dewhirst, J.P. Abraham, J.M. Gorman, E.M. Sparrow, Rationalization of thermal injury quantification methods: application to skin burns, Burns 40 (5) (2014) 896–902, doi:10.1016/j.burns.2013.12.005.
[80] D.E. Haines, Direct measurement of the lethal isotherm for radiofrequency ablation of myocardial tissue, Circ. Arrhythm. Electrophysiol. 4 (5) (2011) e67, doi:10.1161/CIRCEP.111.965459.
[81] Petras A., Leoni M., Guerra J.M., Jansson J., Gerardo-Giorda L. Tissue drives lesion: computational evidence of interspecies variability in cardiac radiofrequency ablation. In: Coudière Y., Ozenne V., Vigmond E., Zemzemi N. (eds) Functional Imaging and Modeling of the Heart. FIMH 2019. Lecture Notes in Computer Science, vol 11504. Springer, Cham.2019 10.1007/978-3-030-21949-9_16.
[82] A. González-Suárez, E. Berjano, Comparative analysis of different methods of modeling the thermal effect of circulating blood flow during RF cardiac ablation, IEEE Trans. Biomed. Eng. 63 (2) (2016) 250–259, doi:10.1109/TBME.2015.2451178.
[83] D.L. Castro-López, M. Trujillo, E. Berjano, R. Romero-Mendez, Two-compartment mathematical modeling in RF tumor ablation: new insight when irreversible changes in electrical conductivity are considered, Math. Biosci. Eng. 17 (6) (2020) 7980–7993, doi:10.3934/mbe.2020405.
[84] C. Rossmanna, D. Haemmerich, Review of temperature dependence of thermal properties, dielectric properties, and perfusion of biological tissues at hyperthermic and ablation temperatures, Crit. Rev. Biomed. Eng. 42 (6) (2014) 467–492, doi:10.1615/critrevbiomedeng.2015012486.
[85] A. González-Suárez, J.J. Pérez, E. Berjano, Should fluid dynamics be included in computer models of RF cardiac ablation by irrigated-tip electrodes? Biomed. Eng. Online 17 (1) (2018) 43 Apr 20, doi:10.1186/s12938-018-0475-7.
[86] C.A. Linte, J.J. Camp, M.E. Rettmann, D. Haemmerich, M.K. Aktas, D.T. Huang, D.L. Packer, D.R. Holmes, Lesion modeling, characterization, and visualization for image-guided cardiac ablation therapy monitoring, J. Med. Imaging (Bellingham) 5 (2) (2018) 021218, doi:10.1117/1.JMI.5.2.021218.
[87] R.T. Roper, M.R. Jones, Benchmark solution for the prediction of temperature distributions during radiofrequency ablation of cardiac tissue, J. Biomech. Eng. 126 (4) (2004) 519–522, doi:10.1115/1.1785810.
[88] C. Parés, E. Berjano, A. González-Suárez, Effect of intracardiac blood flow pulsatility during radiofrequency cardiac ablation: computer modeling study, Int. J. Hyperth. 38 (1) (2021) 316–325, doi:10.1080/02656736.2021.1890240.
[89] Z. Tian, Q. Nan, X. Nie, T. Dong, R Wang, The comparison of lesion outline and temperature field determined by different ways in atrial radiofrequency ablation, Biomed. Eng. Online 15 (Suppl 2) (2016) 124, doi:10.1186/s12938-016-0251-5.
[90] E. Berjano, A. d'Avila, Lumped element electrical model based on three resistors for electrical impedance in radiofrequency cardiac ablation: estimations from analytical calculations and clinical data, Open Biomed. Eng. J. 7 (2013) 62–70, doi:10.2174/1874120720130603001.
[91] H. Nakagawa, F.H. Wittkampf, W.S. Yamanashi, J.V. Pitha, S. Imai, B. Campbell, M. Arruda, R. Lazzara, W.M. Jackman, Inverse relationship between electrode size and lesion size during radiofrequency ablation with active electrode cooling, Circulation 98 (5) (1998) 458–465, doi:10.1161/01.cir.98.5.458.
[92] M. Barkagan, M. Rottmann, E. Leshem, C. Shen, A.E. Buxton, E. Anter, Effect of baseline impedance on ablation lesion dimensions: a multimodality concept validation from physics to clinical experience, Circ. Arrhythm. Electrophysiol. 11 (10) (2018) e006690, doi:10.1161/CIRCEP.118.006690.
[93] I. Babuska, J. Tinsley Oden, Verification and validation in computational engineering and science: basic concepts, Comput. Methods Appl. Mech. Eng. 193 (2004) 4057–4066, doi:10.1016/j.cma.2004.03.002.
[94] M. Viceconti, F. Pappalardo, B. Rodriguez, M. Horner, J. Bischoff, F. Musuamba Tshinanu, *In silico* trials: verification, validation and uncertainty quantification of predictive models used in the regulatory evaluation of biomedical products, Methods 185 (2021) 120–127, doi:10.1016/j.ymeth.2020.01.011.
[95] FDA, Reporting of Computational Modeling Studies in Medical Device Submissions. Guidance for Industry and Food and Drug Administration Staff, U.S. Department of Health and Human Services. Food and Drug Administration, 2016.
[96] Andreuccetti D., Fossi R., Petrucci C. An Internet resource for the calculation of the dielectric properties of body tissues in the frequency range 10 Hz–100 GHz. IFAC-CNR, Florence (Italy), 1997. Based on data published by C.Gabriel et al. in 1996. [Online]. Available: http://niremf.ifac.cnr.it/tissprop/
[97] R.L. Iman, T.A. Cruse, in: Uncertainty and Sensitivity Analyses For Computer Modeling applications. In Reliability technology-1992. The American Society of Mechanical Engineers, Vanderbilt University, 1992, pp. 153–168. (Ed).
[98] I. Rodríguez, J.L. Lequerica, E.J. Berjano, M. Herrero, F. Hornero, Esophageal temperature monitoring during radiofrequency catheter ablation: experimental study based on an agar phantom model, Physiol. Meas. 28 (5) (2007) 453–463, doi:10.1088/0967-3334/28/5/001.
[99] J.L. Lequerica, E.J. Berjano, M. Herrero, L. Melecio, F. Hornero, A cooled water-irrigated intraesophageal balloon to prevent thermal injury during cardiac ablation: experimental study based on an agar phantom, Phys. Med. Biol. 53 (4) (2008) N25–N34, doi:10.1088/0031-9155/53/4/N01.
[100] R. Blasco-Gimenez, J.L. Lequerica, M. Herrero, F. Hornero, E.J. Berjano, Black-box modeling to estimate tissue temperature during radiofrequency catheter cardiac ablation: feasibility study on an agar phantom model, Physiol. Meas. 31 (4) (2010) 581–594, doi:10.1088/0967-3334/31/4/009.
[101] C. Rossmann, A. Motamarry, D. Panescu, D. Haemmerich, Computer simulations of an irrigated radiofrequency cardiac ablation catheter and experimental validation by infrared imaging, Int. J. Hyperth. 38 (1) (2021) 1149–1163, doi:10.1080/02656736.2021.1961027.
[102] M. Wright, E. Harks, S. Deladi, S. Fokkenrood, F. Zuo, A. Van Dusschoten, A.F. Kolen, H. Belt, F. Sacher, M. Hocini, M. Haïssaguerre, P. Jaïs, Visualizing intramyocardial steam formation with a radiofrequency ablation catheter incorporating near-field ultrasound, J. Cardiovasc. Electrophysiol. 24 (12) (2013) 1403–1409.
[103] Q. Zhu, Y. Shen, A. Zhang, L.X. Xu, Numerical study of the influence of water evaporation on radiofrequency ablation, Biomed. Eng. Online 12 (2013) 127, doi:10.1186/1475-925X-12-127.
[104] D.J. Friedman, S.D. Pokorney, A. Ghanem, S. Marcello, I. Kalsekar, S. Yadalam, J.G. Akar, J.V. Freeman, L. Goldstein, R. Khanna, J.P. Piccini, Predictors of cardiac perforation with catheter ablation of atrial fibrillation, JACC Clin. Electrophysiol. 6 (6) (2020) 636–645, doi:10.1016/j.jacep.2020.01.011.
[105] N. Shimko, P. Savard, K. Shah, Radio frequency perforation of cardiac tissue: modelling and experimental results, Med. Biol. Eng. Comput. 38 (5) (2000) 575–582, doi:10.1007/BF02345756.
[106] C.M. Tschabrunn, N.V.K. Pothineni, W.H. Sauer, D. Doynow, J. Salas, T.W. Liao, P. Santangeli, J. Arkles, M.C. Hyman, D.S. Frankel, G.E. Supple, F.C. Garcia, S. Nazarian, S. Dixit, A.E. Epstein, R.D. Schaller, D.J. Callans, F.E. Marchlinski, Evaluation of radiofrequency ablation irrigation type: *in vivo* comparison of normal versus half-normal saline lesion characteristics, JACC Clin. Electrophysiol. 6 (6) (2020) 684–692, doi:10.1016/j.jacep.2020.02.013.
[107] R.M. John, J. Connell, P. Termin, H. Houde-Walter, G. Eberl, K.M. Stohlman, M.G. Curley, Characterization of warm saline-enhanced radiofrequency ablation lesions in the infarcted porcine ventricular myocardium, J. Cardiovasc. Electrophysiol. 25 (3) (2014) 309–316, doi:10.1111/jce.12307.
[108] R. Barauskas, A. Gulbinas, G. Barauskas, Finite element modeling and experimental investigation of infiltration of sodium chloride solution into nonviable liver tissue, Med. (Kaunas). 43 (5) (2007) 399–411.
[109] J.Z. Tsai, J.A. Will, S. Hubbard-Van Stelle, H. Cao, S. Tungjitkusolmun, Y.B. Choy, D. Haemmerich, V.R. Vorperian, J.G. Webster, *In-vivo* measurement of swine myocardial resistivity, IEEE Trans. Biomed. Eng. 49 (5) (2002) 472–483, doi:10.1109/10.995686.
[110] N.C. Bhavaraju, J.W Valvano, Thermophysical properties of swine myocardium, Int. J. Thermophys. 20 (1999) 665–676, doi:10.1023/A:1022673524963.
[111] A. Bhattacharya, R.L. Mahajan, Temperature dependence of thermal conductivity of biological tissues, Physiol. Meas. 24 (3) (2003) 769–783, doi:10.1088/0967-3334/24/3/312.
[112] M. Pop, A. Molckovsky, L. Chin, M.C. Kolios, M.A. Jewett, M.D. Sherar, Changes in dielectric properties at 460 kHz of kidney and fat during heating: importance for radio-frequency thermal therapy, Phys. Med. Biol. 48 (15) (2003) 2509–2525, doi:10.1088/0031-9155/48/15/317.
[113] D. Deas Yero, F. Gilart Gonzalez, D. Van Troyen, G.A.E. Vandenbosch, Dielectric Properties of Ex Vivo Porcine Liver Tissue Characterized at Frequencies Between 5 and 500 kHz When Heated at Different Rates, IEEE Trans. Biomed. Eng. 65 (11) (2018) 2560–2568, doi:10.1109/TBME.2018.2807981.
[114] N.C. Bhavaraju, H. Cao, D.Y. Yuan, J.W. Valvano, J.G. Webster, Measurement of directional thermal properties of biomaterials, IEEE Trans. Biomed. Eng. 48 (2) (2001) 261–267, doi:10.1109/10.909647.
[115] V. Jacquemet, Lessons from computer simulations of ablation of atrial fibrillation, J. Physiol. 594 (9) (2016) 2417–2430, doi:10.1113/JP271660.
[116] P.M. Boyle, S. Zahid, N.A. Trayanova, Towards personalized computational modelling of the fibrotic substrate for atrial arrhythmia, Europace 18 (suppl 4) (2016), doi:10.1093/europace/euw358.
[117] C. Wei, P.C. Qian, M. Boeck, J.S. Bredfeldt, R. Blankstein, U.B. Tedrow, R. Mak, P.C. Zei, Cardiac stereotactic body radiation therapy for ventricular tachycardia: current experience and technical gaps, J. Cardiovasc. Electrophysiol. 32 (11) (2021) 2901–2914, doi:10.1111/jce.15259.

[118] N. Cedilnik, J. Duchateau, R. Dubois, F. Sacher, P. Jaïs, H. Cochet, M. Sermesant, Fast personalized electrophysiological models from computed tomography images for ventricular tachycardia ablation planning, Europace 20 (suppl_3) (2018) iii94–iii101, doi:10.1093/europace/euy228.
[119] R. Rordorf, A. Sanzo, V. Gionti, Contact force technology integrated with 3D navigation system for atrial fibrillation ablation: improving results? Expert Rev. Med. Devices 14 (6) (2017) 461–467, doi:10.1080/17434440.2017.1330149.
[120] B. Schumacher, O. Eick, F. Wittkampf, C. von Pezold, J. Tebbenjohanns, W. Jung, B. Lüderitz, Temperature response following nontraumatic low power radiofrequency application, Pacing Clin. Electrophysiol. 22 (2) (1999) 339–343, doi:10.1111/j.1540-8159.1999.tb00448.x.
[121] D. Haemmerich, J.P. Saul, Quantification of local convectional cooling during cardiac radiofrequency catheter ablation, in: Proceedings of the Annual International Conference of the IEEE Engineering in Medicine and Biology Society, 2006, IEEE, 2006, pp. 6293–6296, doi:10.1109/IEMBS.2006.259993.
[122] M. Zaltieri, C. Massaroni, F.M. Cauti, E. Schena, Techniques for temperature monitoring of myocardial tissue undergoing radiofrequency ablation treatments: an overview, Sens. (Basel) 21 (4) (2021) 1453, doi:10.3390/s21041453.
[123] A. Koh, S.R. Gutbrod, J.D. Meyers, C. Lu, R.C. Webb, G. Shin, Y. Li, S.K. Kang, Y. Huang, I.R. Efimov, J.A. Rogers, Ultrathin injectable sensors of temperature, thermal conductivity, and heat capacity for cardiac ablation monitoring, Adv. Healthc. Mater. 5 (3) (2016) 373–381, doi:10.1002/adhm.201500451.
[124] D.M. Nguyen, T. Andersen, P. Qian, T. Barry, A. McEwan, Electrical Impedance Tomography for monitoring cardiac radiofrequency ablation: a scoping review of an emerging technology, Med. Eng. Phys. 84 (2020) 36–50, doi:10.1016/j.medengphy.2020.07.025.
[125] D.M. Nguyen, P. Qian, T. Barry, A. McEwan, Cardiac radiofrequency ablation tracking using electrical impedance tomography, Biomed. Phys. Eng. Express 6 (1) (2020) 015015, doi:10.1088/2057-1976/ab5ce8.
[126] E. Ghafoori, E.G. Kholmovski, S. Thomas, J. Silvernagel, N. Angel, N. Hu, D.J. Dosdall, R. MacLeod, R. Ranjan, Characterization of gadolinium contrast enhancement of radiofrequency ablation lesions in predicting edema and chronic lesion size, Circ. Arrhythm. Electrophysiol. 10 (11) (2017) e005599, doi:10.1161/CIRCEP.117.005599.